

Differentiable Bilevel Programming for Stackelberg Congestion Games

Jiayang Li¹ Jing Yu¹ Qianni Wang¹ Boyi Liu²
 Zhaoran Wang² Yu (Marco) Nie^{1,*}

September 19, 2022

Abstract

A Stackelberg congestion game (SCG) is a bilevel program in which a leader aims to maximize their own gain by anticipating and manipulating the equilibrium state at which followers settle by playing a congestion game. Large-scale SCGs are well known for their intractability and complexity. This study approaches SCGs through differentiable programming, which marries the latest developments in machine learning with conventional methodologies. The core idea centers on representing the lower-level equilibrium problem using an evolution path formed by the imitative logit dynamics. It enables the use of automatic differentiation over the evolution path towards equilibrium, leading to a double-loop gradient descent algorithm. We further show the fixation on the lower-level equilibrium may be a self-imposed computational obstacle. Instead, the leader may only look ahead along the followers’ evolution path for a few steps, while updating their decisions in sync with the followers through a co-evolution process. The revelation gives rise to a single-loop algorithm that is more efficient in terms of both memory consumption and computation time. Through numerical experiments that cover a wide range of benchmark problems, we find the single-loop algorithm consistently strikes a good balance between solution quality and efficiency, outperforming not only the standard double-loop implementation but also other methods from the literature. Importantly, our results highlight both the wastefulness of “full anticipation” and the peril of “zero anticipation”. If a quick-and-dirty heuristic is needed for solving a really large SCG, the proposed single-loop algorithm with a one-step look-ahead makes an ideal candidate.

Keywords: automatic differentiation, bilevel programming, differentiable programming, imitative logit dynamics, machine learning, Stackelberg congestion game

1 Introduction

In a Stackelberg game (von Stackelberg, 1952; Sherali et al., 1983), a leader aims to maximize their own gain by manipulating the self-interested followers of the game. Such a game has a natural *bilevel* hierarchy. At the upper level, the leader’s decision is contingent upon the response of the followers, whereas at the lower level, the response of the followers is regulated by that very decision. Many transportation management problems can be framed as a Stackelberg game in which a leader aims to improve the performance of a transportation system used by travelers (followers). These problems range from congestion pricing (Dafermos, 1973; Smith, 1979b; Verhoef, 2002; Friesz et al., 2004; Simoni et al., 2019; Li et al., 2021) and network design

¹Department of Civil and Environmental Engineering, Northwestern University, Evanston, IL 60208, USA. ²Department of Industrial Engineering and Management Science, Northwestern University, Evanston, IL 60208, USA. *Corresponding author; email: y-nie@northwestern.edu.

(Leblanc, 1975; Smith, 1979c; Marcotte and Marquis, 1992; Yang and H. Bell, 1998; Meng et al., 2001; Zhang et al., 2009; Li et al., 2012) to traffic control (Gartner, 1985; Improtta, 1987; Cantarella and Sforza, 1987; Smith and Van Vuren, 1993; Peeta and Mahmassani, 1995; Yang et al., 2007; Xiao and Lo, 2015). In transportation management, the followers’ best response is usually characterized as a Wardrop equilibrium (WE) of a congestion game, which dictates no traveler can reduce their travel time by adjusting travel choices unilaterally (Wardrop, 1952). Hence, a *Stackelberg congestion game* (SCG), the focus of the present study, is equivalent to a bilevel program constrained by an equilibrium problem (Luo et al., 1996).

Stackelberg games are generally difficult to solve due to their bilevel hierarchy. If the leader hopes to improve their current decision, they need to calculate the derivative of their objective function with respect to that decision, which in turn requires examining the sensitivity of the best response of the followers (i.e., the WE of the congestion game). However, accurately performing this sensitivity analysis is a computational challenge that has not been satisfactorily addressed, especially in large-scale applications. For one thing, a congestion game may have multiple equilibria (Bahrami and Roorda, 2020). When more than one equilibrium exists, the leader is forced to pick one, which often entails another layer of hierarchy (Bar-Gera and Luzon, 2007). However, the leader’s control over the actual equilibrium state in the lower level is by no means absolute since the followers have the freedom to choose. Thus, to imagine the leader can pick a preferred equilibrium is a bit of wishful thinking. Moreover, even when uniqueness is guaranteed, analyzing the sensitivity of this equilibrium is still not amenable to efficient computation in general. In the literature, it is often carried out *implicitly* on the equilibrium conditions (Tobin, 1986; Tobin and Friesz, 1988), which typically requires storing and inverting (large) matrices.

Recently, the machine learning (ML) community has discovered a range of new applications of bilevel programming, e.g., hyperparameter tuning (Maclaurin et al., 2015) and neural architecture search (Liu et al., 2018). A common feature in the bilevel programs derived from these ML applications is that their lower level is a deep learning problem (LeCun et al., 2015; Goodfellow et al., 2016). In other words, they can be interpreted as a Stackelberg game in which the follower trains a deep neural network (DNN) *according to the instruction of a leader*. This means the leader knows the process through which the follower achieves the best response, and can express it *explicitly* through *that* process as a mapping of the leader’s decision. Take neural architecture search (Liu et al., 2018) for example. The goal is to find the optimal DNN architecture for a learning task. It can be viewed as a Stackelberg game in which a leader designs the DNN structure while the follower trains the DNN accordingly. The best response of the follower — a local solution to the deep learning problem — is the output of the training process. Since this process is coded as a numeric computer program, the leader can evaluate the gradient of their objective function by *differentiable programming*, a computational paradigm that finds the gradient of an algorithmic structure based on automatic differentiation (AD) (Baydin et al., 2018). AD exploits the fact that a computer program, however complicated as it may be, can be decomposed into a sequence of elementary arithmetic operations and functions. By applying the chain rule repeatedly to these operations and functions, the derivative of the program’s outputs with respect to any inputs can be computed automatically, using a number of arithmetic operations tightly bound by that required to produce the output for the original program (Griewank et al., 1989). The concept of differential programming is general and flexible. For example, DNN itself is a differentiable program (DiP). In fact, the ability to quickly *unroll* — or differentiate through — extremely complex DNN using AD was a key to the success of the modern ML enterprise (Rumelhart et al., 1986; LeCun et al., 1996). However, an algorithm that trains a DNN may also be treated as a DiP, and hence be similarly “unrolled”. Having witnessed the power of differentiable programming in tackling ML-inspired applications, one naturally wonders whether that power can be harnessed to meet the challenges posed by SCGs. In this study, we set out to answer that question.

First and foremost, we propose to cast a WE as a DiP. The idea is straightforward but relatively new: an iterative process through which the followers in an SCG arrive at such an equilibrium may be described using a DiP. This process may be an algorithm devised to find the equilibrium or a set of rules that defines the choice behaviors of the followers. However, not every algorithm, nor every set of behavioral rules, can be cast as a DiP. [Li et al. \(2020\)](#) show the projection algorithm is differentiable because each projection operation can be reformulated as a quadratic program (QP), which is known to be a DiP ([Amos and Kolter, 2017](#); [Agrawal et al., 2019](#)). Theirs is the first attempt, to the best of our knowledge, to solve SCG through differentiable programming. In this study, we take an alternative approach that expresses a WE as the limit point of an evolutionary game specified by the followers’ choice behaviors ([Smith, 1979a](#); [Weibull, 1997](#)). This concept is similar to the day-to-day dynamical process widely studied in the transportation literature ([Cascetta and Cantarella, 1991](#); [Smith and Wisten, 1995](#); [Watling and Hazelton, 2003](#); [Xiao et al., 2019](#)). We adopt the imitative logit dynamics (ILD) ([Björnerstedt and Weibull, 1994](#)), which not only offers a simple but sensible behavioral interpretation but also provably converges to a WE under weak conditions. We shall show that ILD can be programmed as a DiP whose structure is similar to a DNN. The hidden layers of this DNN map the followers’ choice from one day (a.k.a stage) to the next, based on their experienced utility on that day. Meanwhile, the leader’s decision can be embedded in these layers, as *weights* or trainable parameters. Then, given an initial state, the DNN constructed in this manner can predict the followers’ choice and the leader’s payoff on each day, and more importantly, calculate the gradient of these outputs with respect to any parameters via AD, very much like the process of training a DNN ([LeCun et al., 1996](#)). Our work verifies that under the proposed framework, the ratio between the cost of calculating the gradient of the leader’s payoff on each day and the cost of evaluating that payoff is a small constant.

Second, we develop two new algorithms for solving SCGs based on AD. The first is a gradient descent algorithm implemented with differential programming. In each iteration, it runs the evolutionary dynamics until convergence, before calculating the gradient of the leader’s cost through AD. The leader’s decision is then updated using the gradient information and sent back to the lower level to start another iteration. Although the overall structure of the algorithm is similar to conventional sensitivity-analysis (or implicit differentiation) based methods, it enjoys better scalability and greater efficiency thanks to AD. However, finding WE could create computational graphs (DNN) too “deep” to unroll efficiently even with AD. This inefficiency severely hinders the applicability of the algorithm on large-scale and/or highly “congested” problems for which equilibration tends to take many iterations. Motivated by this difficulty, our second algorithm takes an evolutionary rather than equilibrium approach to interpreting the followers’ behaviors. That is, instead of anticipating the followers’ response at equilibrium, the leader may only look ahead along the followers’ evolution path for a few steps. With such *limited anticipation*, the leader need not wait until the followers settle at a new equilibrium to correct course. Instead, the two parties can *co-evolve*, meaning they each update decisions simultaneously in every step of a shared evolution process. Short-term anticipation limits the depth of the computational graph through which the gradient of the leader’s objective is evaluated. Co-evolution, on the other hand, breaks the bilevel hierarchy and turns the solution process into a single loop. Taken together, they consistently deliver computational performance orders of magnitude better than the benchmarks, including the first algorithm, as demonstrated by numerical experiments. The second algorithm is not just much faster. We shall show through numerical experiments it consistently provides high-quality approximate solutions.

Differentiable bilevel programming based on evolutionary dynamics offers a flexible and generalizable approach to tackling a wide range of SCGs. For one thing, it is not fixated on a particular definition of equilibrium. Other types of equilibria can be incorporated as long as they are the limit of an evolutionary

dynamical process. In fact, even an dynamical process not associated with any stable equilibrium can still be a valid and practically useful behavioral representation in a real-world SCG problem. The proposed approach can also handle complex equilibrium settings — such as user heterogeneity and asymmetric interactions — with ease. This advantage is conferred by replacing equilibrium conditions with a dynamical process that operates on the zeroth order (i.e., it requires no more information than the followers’ utility).

The rest of the paper is organized as follows. Section 2 discusses related studies. Section 3 covers the basics of automatic differentiation and mirror descent. Section 4 provides a general formulation of SCG as a bilevel program. Section 5 introduces the ILD and establishes convergence conditions that are weaker than known results. Section 6 explains how to unroll the ILD through AD and analyzes the complexity of the procedure. Section 7 proposes two AD-based algorithms for solving SCGs, and in Section 8, we discuss how the proposed approach may be extended to more general settings. Results of numerical experiments are reported in Section 9. Section 10 concludes the paper with a summary of main results and directions for further research.

1.1 Notation

We use \mathbb{R} and \mathbb{R}_+ to denote the set real numbers and non-negative real numbers. For a vector $\mathbf{a} \in \mathbb{R}^n$, we denote its ℓ_1 , ℓ_2 and ℓ_∞ norms as $\|\mathbf{a}\|_1$, $\|\mathbf{a}\|_2$ and $\|\mathbf{a}\|_\infty$. For a vector $\mathbf{a} \in \mathbb{R}^n$, we denote $\text{supp}(\mathbf{a}) = \{i : a_i > 0\}$ as its support. For two vectors $\mathbf{a}, \mathbf{b} \in \mathbb{R}^n$, their inner product and outer product are denoted as $\langle \mathbf{a}, \mathbf{b} \rangle$ and $\mathbf{a} \otimes \mathbf{b}$, respectively. The element-wise multiplication and division between \mathbf{a} and \mathbf{b} is denoted as $\mathbf{a} \circ \mathbf{b}$ and \mathbf{a}/\mathbf{b} , respectively. For a matrix $\mathbf{A} \in \mathbb{R}^{n \times m}$, we write $\text{nnz}(\mathbf{A})$ as the number of nonzero elements in matrix \mathbf{A} . For a finite set \mathbb{A} , we write $|\mathbb{A}|$ as the number of elements in \mathbb{A} and $2^{\mathbb{A}}$ as the set of all subsets of \mathbb{A} . For two matrices $\mathbf{A} \in \mathbb{R}^{n_1 \times n_2}$ and $\mathbf{B} \in \mathbb{R}^{n_2 \times n_3}$, we use \mathbf{AB} to represent matrix multiplication. In pseudo-codes, for two variables a and b , we use $a += b$ to represent the operation $a \leftarrow a + b$.

2 Related Work

Our study lies at the nexus of several areas scattered in different domains. We start by examining transportation management problems (Section 2.1), which serve as the primary motivation. Section 2.2 discusses conventional algorithms for Stackelberg games, including those capable of finding global solutions and those promising only local solutions. In Section 2.3, we discuss several heuristics that seek to find approximate solutions by relaxing or transforming Stackelberg congestion games (SCGs) into a simpler problem. Section 2.4 covers the recent applications of AD in solving ML-inspired bilevel programs. We end this section with a brief review of evolutionary games (Section 2.5).

2.1 Transportation Management Problems

It has long been recognized that the selfish choice of travelers contributes to excessive traffic congestion (Beckmann et al., 1956; Sheffi, 1985). Selfish travelers, seeking to minimize *their own* travel cost, would settle at a Wardrop equilibrium (WE) (Wardrop, 1952). This equilibrium state, however, is sometimes inefficient as it may lead to a higher travel cost than the minimum possible (Braess, 1968; Roughgarden and Tardos, 2002). Hence, the basic rationale behind transportation management is to close the gap between these two states, which typically requires cooperation orchestrated by a central manager. Extensive research efforts

have been devoted to transportation management problems since the late 1970s (Smith, 1979c; Gartner, 1985; Smith and Van Vuren, 1993; Peeta and Mahmassani, 1995; Friesz et al., 2004; Smith and Mounce, 2011; Xiao and Lo, 2015).

The recent development in the space of connected and autonomous vehicles (CAV) has stimulated renewed interest in this topic (Mahmassani, 2016). A popular management strategy concerns dedicated CAV facilities (Chen et al., 2016, 2017; Bahrami and Roorda, 2020), and controlling CAVs within such facilities (Levin and Boyles, 2016; Talebpour et al., 2017; Lu et al., 2019). The idea is that the system throughput may be increased by physically separating CAVs from human-driven vehicles (HDV). Another stream of research aims to influence the travel choice of CAVs, directly or indirectly. The direct approach dictates the travel choice (e.g., routes) of a CAV fleet to achieve certain system objectives (Zhang and Nie, 2018; Bıyık et al., 2018; Sharon et al., 2018; Li et al., 2018; Chen et al., 2020). The promise is that, by controlling but a small portion of CAV traffic flow in this centralized fashion, one can eliminate most of the efficiency losses (Zhang and Nie, 2018; Sharon et al., 2018; Chen et al., 2020). The indirect approach, on the other hand, attempts to manage travel demand by providing incentives. The most widely studied scheme in this category derives from congestion pricing (Vickrey, 1969; Dafermos, 1973; Smith, 1979b; Verhoef, 2002; Simoni et al., 2019; Li et al., 2021). With CAVs it is possible to charge HDVs and CAVs a different toll even when they share the same road facility, a practice known as discriminatory pricing. Several recent studies (Mehr and Horowitz, 2019; Lazar et al., 2019; Delle Site, 2021) examined the toll design problem in this context.

2.2 Conventional Algorithms for Stackelberg Games

The most straightforward method for solving a Stackelberg game is to reformulate it as a bilevel program. In the optimization literature, global algorithms for bilevel programs, e.g., vertex enumeration (Candler and Townsley, 1982; Bialas and Karwan, 1984), branch-and-bound, (Bard and Falk, 1982; Bard, 1988; Al-Khayyal et al., 1992) and complementary pivoting (Bialas et al., 1980), are usually only applicable when the upper level is linear and the lower level is linear or convex quadratic. For more general bilevel programs such as those arising from transportation management, the focus is to find local solutions. These local algorithms have many variants, but in general, they can be classified as either basic gradient descent methods (Friesz et al., 1990; Yang, 1995), steepest descent methods built on quadratic approximation (Luo et al., 1996), or penalty function methods (Aiyoshi and Shimizu, 1984; Ishizuka and Aiyoshi, 1992). The reader is referred to Colson et al. (2007) for a comprehensive review of both global and local algorithms. Below we focus on the gradient descent method because that is the point of departure of this investigation.

To calculate the gradient of a bilevel program, one first needs to calculate the Jacobian matrix of the lower-level solution with respect to the upper-level decision variables. A classical approach to this problem relies on the implicit differentiation theorem (Tobin, 1986; Dafermos, 1988; Tobin and Friesz, 1988). One way to apply the theorem is to represent the lower-level problem as a variational inequality problem (VIP), which can be transformed into a fixed-point problem using a Euclidean projection (EP) operator (Nagurney, 2013). The Jacobian matrix is then obtained by implicitly differentiating the fixed-point problem. This approach requires inverting a matrix whose size scales quadratically with that of the lower-level decision variables. As SCGs in transportation management are defined over road networks and the decision variables in the lower-level problems are often related to paths used at equilibrium, the matrix needed to be inverted can be very large in applications of practical significance. For networks with tens of thousands of links, just storing such matrices explicitly may be impractical, let alone performing inversion operations on them. Of course, a more daunting challenge arises when the lower-level problem fails to admit a unique solution. In

this case, the implicit differentiation theorem is no longer applicable. Indeed, it is well known that WE in SCGs from transportation management is not unique in terms of path flows. [Tobin and Friesz \(1988\)](#) devised an implicit differentiation scheme relying on a specific equilibrium path flow that is a nondegenerate extreme point of the solution set. However, finding such a solution is an extra burden to an already computationally intensive method. Alternatively, [Patriksson and Rockafellar \(2002\)](#) suggested one may directly differentiate the equilibrium conditions in the space of link flows to bypass the curse of multiple equilibria. However, even link flows may not be unique, if more complex settings, such as user heterogeneity and asymmetric link interactions, are considered.

In this study, we shall attempt to kill two birds — avoiding unscalable matrix operations and bypassing the difficulty posed by multiple equilibria — with one stone: gradient descent algorithms based on AD and evolutionary dynamics.

2.3 Approximation Heuristics for Stackelberg Congestion Games

Inspired by the inherent difficulty in solving bilevel programs, many heuristic methods have been proposed to approximate SCGs. These methods may be roughly classified into three categories (see [Migdalas, 1995](#), Section 3.2 for an overview). The first assumes the followers and the leader work cooperatively to achieve the same objective ([Dantzig et al., 1979](#)), thus reducing the SCG to a single-level system optimum problem. In the second category, the upper- and lower-level problems are merged together by forcing the followers to account for the leader’s objective in their decision. As a result, the SCG is simplified as a congestion game in which players’ utility is distorted by a term related to a system objective ([Poorzahedy and Turnquist, 1982](#)). Neither of the above methods guarantees to secure a feasible solution to the original SCG.

The most popular is perhaps the third heuristic, which assumes the leader and the followers compete à la [Cournot \(1897\)](#). In other words, it approximates a Stackelberg game with a Cournot game. To solve a Cournot game, one simply finds the best response of the leader and the followers iteratively while fixing each other’s decisions, also known as the iterative optimization-assignment (IOA) scheme ([Marcotte and Marquis, 1992](#)). With suitable regularity conditions, the iterative process ends at a Nash-Cournot equilibrium at which neither the leader nor the followers can unilaterally improve their prospects ([Fisk, 1984](#)). As it eliminates the dependency of the lower-level solution on the upper-level decision variables, this heuristic bypasses the calculation of the lower-level solution’s Jacobian all together. Hence, its complexity — regardless of the implementation details — is a linear, rather than a quadratic, function of the sizes of the upper- and lower-level decision variable. The Cournot approximation has been used by many researchers for solving SCGs ([Tan et al., 1979](#); [Marcotte, 1983, 1986](#); [Friesz and Harker, 1985](#); [Fisk, 1986](#); [Yang et al., 1992](#)), and it has delivered a satisfactory performance to many applications. However, the gap between the Nash-Cournot equilibrium and the solution to the SCG can become unacceptable, if the followers’ optimal choice at equilibrium is sensitive to the leader’s decision. The co-evolution algorithm proposed in this paper can be viewed as a refinement of this heuristic.

2.4 ML-Inspired Bilevel Programs

Bilevel programming has found many applications in ML lately, ranging from hyperparameter optimization ([Maclaurin et al., 2015](#); [Franceschi et al., 2018](#)) and model-agnostic meta-learning ([Finn et al., 2017](#)) to adversarial learning ([Tian et al., 2020](#)) and neural architecture search ([Liu et al., 2018](#)). The lower-level

problem in these bilevel programs is a deep learning problem (typically cast as an unconstrained optimization problem). In the ML literature, these problems are often solved by various gradient descent algorithms, which evaluate the gradient either through implicit differentiation or AD (Grazzi et al., 2020). The reader is referred to Liu et al. (2021) for a recent review. The AD-based approach is a natural choice in the ML community. Its use in more traditional application domains of bilevel programs, however, is rather limited.

The AD-based approach treats the algorithm for solving the deep learning problem — or training a deep neural network, to use the ML terminology — as a DiP. When unrolling this training process, AD may be carried out fully (e.g., Franceschi et al., 2017, 2018) or partially (e.g., Shaban et al., 2019). In both cases, the lower-level learning problem is solved exactly at first. This is often known as the *forward pass*. The difference between the full and the partial unrolling lies in the *backward pass*. Whereas full AD always unrolls the entire training process, partial AD “truncates” it, i.e., unrolls only the last portion. Truncation improves computational efficiency but may undermine the accuracy of the gradient evaluation. Pushing the idea of truncation to extreme yields a method called one-stage AD (e.g., Liu et al., 2018; Xu et al., 2019), which updates upper and lower levels simultaneously in a single loop. Specifically, whenever the trainable parameters in the learning problem are updated by one gradient-descent step, the algorithm unrolls it to obtain a gradient for updating the upper-level decisions. Although the method performs well on many tasks (e.g., Luketina et al., 2016; Metz et al., 2016; Finn et al., 2017; Liu et al., 2018), its analytical properties have not been fully explored.

Inspired by the AD-based approach in ML, Li et al. (2020) explored its application in SCGs. Their algorithm unrolls a Euclidean projection (EP) method (Dafermos, 1983) for solving the lower-level equilibrium problem. It casts each projection iteration as a quadratic program (QP), which is known to be a DiP (Amos and Kolter, 2017). Taken together, the lower-level solution process can be interpreted as a DNN whose layers correspond to the projection iterations. The gradient is then evaluated by unrolling through the DNN via standard AD. The algorithms proposed in this paper build on Li et al. (2020) but cast the lower-level solution process as ILD drawn from evolutionary game theory.

2.5 Evolutionary Games

The study of evolutionary games (Weibull, 1997) can be traced back to the equilibrium selection problem (Harsanyi et al., 1988), which aims to explain why the players of a game would commit to a certain equilibrium when the game has more than one solution. Underlying the evolutionary game theory is the idea that the equilibrium “selected” by the players can be written as a *function* of the equilibration process through which it is achieved. In the literature, numerous evolutionary dynamics have been proposed to describe this equilibration process (see e.g. Sandholm, 2015, for an overview). In transportation, evolutionary dynamics, in various forms, have been used to model and interpret WE and its generalizations (see e.g., Smith, 1984; Friesz et al., 1994; Zhang and Nagurney, 1996; Watling, 1999; Han and Du, 2012; Zhang et al., 2015; Xiao et al., 2019), although it is often known as the day-to-day (DTD) dynamical process.

Imitative dynamics (with the ILD as a special case), first proposed by Björnerstedt and Weibull (1994), is one of the most widely-used evolutionary dynamics. It models the players’ behavior with a simple rule: they learn to adapt their strategies by imitating previous successful experiences. Our work establishes the convergence of ILD in congestion games by interpreting the ILD as the outcome of all travelers simultaneously minimizing their expected costs by a special mirror descent (MD) method (Nemirovskij and Yudin, 1983). Although this convergence result, to the best of our knowledge, is new, its connections to known results in the literature

warrant explanations. The convergence of MD for convex programs has been extensively studied (see e.g., Doan et al., 2018; Radhakrishnan et al., 2020, and the references therein). However, these convergence results are only applicable to congestion games that have an equivalent optimization problem. In the transportation literature, it is well known that a congestion game cannot be formulated as an optimization problem when there exist asymmetric interactions between flows on different links or in different classes (Bahrami and Roorda, 2020). Our result is not subject to this limitation. A few recent studies also studied the convergence of the MD method for games. Mertikopoulos and Zhou (2019), for example, analyze the convergence of MD in games with continuous action sets. More relevant is Krichene et al. (2015), which establishes the MD method’s convergence in routing games. However, their convergence analysis assumes a condition that the ILD does not satisfy. Finally, to ensure convergence, most previous studies require the learning rate progressively decrease (Krichene et al., 2015; Doan et al., 2018). Our result is stronger because it asserts a fixed learning rate also ensures convergence in congestion games.

3 Preliminary

In this section, we introduce two foundational methods, automatic differentiation (Section 3.1) and mirror descent (Section 3.2), which are the cornerstones for our differentiable bilevel programming approach.

3.1 Automatic Differentiation

Automatic differentiation (AD) is used to numerically evaluate functions $f : \mathbb{R}^m \rightarrow \mathbb{R}^n$. It can be carried either in a *forward mode* or a *reverse mode*. Which mode is preferable depends on m/n . If the ratio is very small (large), the forward (reverse) model is more efficient and hence preferred. In this paper, we only focus on the reverse mode because f is always a scalar function (i.e., $n = 1$) in the applications relevant to our main interest. In reverse-mode AD, derivatives are computed in two phases. In the first — often known as the *forward propagation* (FP) — phase, the function is evaluated, and intermediate variables and their inter-dependencies are stored in a computational graph. In the second — or the *backward propagation* (BP) — phase, the derivatives of all intermediate variables (including the outputs of the function) are evaluated in a reverse order based on the chain rule defined by the inter-dependencies. Below we explain how it works with an ML example.

Example 3.1 (AD for deep learning). *Consider a DNN $g : \mathbb{R}^n \times \mathbb{R}^{n \times n \times 3} \times \mathbb{R}^{n \times 3} \rightarrow \mathbb{R}^n$ with three fully-connected layers of the following form*

$$g(\mathbf{x}; \{\mathbf{W}^i\}_{i=0}^2, \{\mathbf{b}^i\}_{i=0}^2) = f(\mathbf{W}^2 + f(\mathbf{W}^1 + f(\mathbf{W}^0 \mathbf{x} + \mathbf{b}^0) + \mathbf{b}^1) + \mathbf{b}^2), \quad (3.1)$$

where the activation function $f : \mathbb{R}^n \rightarrow \mathbb{R}^n$ is an element-wise \tanh function. Suppose the DNN is trained with a data pair $(\mathbf{x}^{\text{train}}, \mathbf{y}^{\text{train}})$ to minimize a squared error that reads

$$l = \frac{1}{2} \cdot \|g(\mathbf{x}^{\text{train}}; \{\mathbf{W}^i\}_{i=0}^2, \{\mathbf{b}^i\}_{i=0}^2) - \mathbf{y}^{\text{train}}\|_2^2.$$

Central to the training process is to compute the gradients of function $l(\{\mathbf{W}^i\}_{i=0}^2, \{\mathbf{b}^i\}_{i=0}^2)$ with respect to \mathbf{W}^i and \mathbf{b}^i , i.e., $\bar{\mathbf{W}}^i = \partial l / \partial \mathbf{W}^i$ and $\bar{\mathbf{b}}^i = \partial l / \partial \mathbf{b}^i$ ($i = 0, 1, 2$). Reverse-mode AD first evaluates function l as described in Algorithm 1. Then it calculates the gradients of l in a backward propagation (see Algorithm 2). Note that, in Algorithm 2, any symbol with a bar accent represents a derivative of l with respect to the

symbol without the accent. For example, applying the chain rule to line 4 in Algorithm 1 yields, noting $f'(x) = 1 - (f(x))^2$ since $f(x) = \tanh(x)$,

$$\bar{\mathbf{a}}^i = f'(\mathbf{a}^i) \cdot \frac{\partial l}{\partial \mathbf{x}^{i+1}} = (\mathbf{1} - (f(\mathbf{a}^i))^2) \circ \frac{\partial l}{\partial \mathbf{x}^{i+1}} = (\mathbf{1} - (\mathbf{x}^{i+1})^2) \circ \bar{\mathbf{x}}^{i+1},$$

which is precisely line 3 in Algorithm 2. Clearly, AD allows the derivative with respect to any intermediate variable to be evaluated in a single backward pass.

Algorithm 1 FP for deep learning.

```

1:  $\mathbf{x}^0 = \mathbf{x}^{\text{train}}$ 
2: for  $i = 0, 1, 2$  do
3:    $\mathbf{a}^i = \mathbf{W}^i \mathbf{x}^i + \mathbf{b}^i$ 
4:    $\mathbf{x}^{i+1} = f(\mathbf{a}^i)$ 
5: end for
6:  $l = 1/2 \cdot \|\mathbf{x}^3 - \mathbf{y}^{\text{train}}\|_2^2$ 
```

Algorithm 2 BP for deep learning.

```

1:  $\bar{\mathbf{x}}^3 = \mathbf{x}^3 - \mathbf{y}^{\text{train}}$ 
2: for  $i = 2, 1, 0$  do
3:    $\bar{\mathbf{a}}^i = (\mathbf{1} - (\mathbf{x}^{i+1})^2) \circ \bar{\mathbf{x}}^{i+1}$ 
4:    $\bar{\mathbf{W}}^i = \mathbf{x}^i \otimes \bar{\mathbf{a}}^i$  and  $\bar{\mathbf{b}}^i = \bar{\mathbf{a}}^i$ 
5: end for
6:  $\bar{\mathbf{x}}^{\text{train}} = \bar{\mathbf{x}}^0$ 
```

Linnainmaa (1970) is often credited with the first formal description of reverse-mode AD, whereas the first machine-based implementation of reverse-mode AD was proposed by Speelpenning (1980). In a machine-based implementation, one only needs to define the computational graph through FP, and BP is always left to the machine to program automatically. Most modern deep learning frameworks, e.g., Theano (Al-Rfou et al., 2016), TensorFlow (Abadi et al., 2016), PyTorch (Paszke et al., 2019), and JAX (Frostig et al., 2018), are equipped with machine-based AD.

3.2 Mirror Descent

The mirror descent (MD) method was initially introduced as a generalization of the projected gradient descent method (Nemirovskij and Yudin, 1983). Similar to the projected gradient descent method, the MD method seeks to diminish the “distance” between two successive iterations. The difference is the MD method defines the distance using *Bregman divergence*, which is more general than the Euclidean distance used by the projected gradient descent method.

Definition 3.2 (Bregman divergence). Let \mathbb{X} be a closed convex set and $\phi : \mathbb{X} \rightarrow \mathbb{R} \cup \{\infty\}$ be a strongly convex and continuously differentiable function. Then for all $\mathbf{x} \in \mathbb{X}$ and $\mathbf{x}' \in \mathbb{X}$, the Bregman divergence $D_\phi(\mathbf{x}, \mathbf{x}')$ induced by ϕ between \mathbf{x} and \mathbf{x}' is defined as

$$D_\phi(\mathbf{x}, \mathbf{x}') = \phi(\mathbf{x}) - \phi(\mathbf{x}') - \langle \nabla \phi(\mathbf{x}'), \mathbf{x} - \mathbf{x}' \rangle. \quad (3.2)$$

Consider the problem of minimizing a continuous differentiable and convex function $f : \mathbb{X} \rightarrow \mathbb{R}$ over a convex set $\mathbb{X} \subseteq \mathbb{R}^n$. At the current iteration $\mathbf{x}^t \in \mathbb{X}$, the MD method finds the next iterate \mathbf{x}^{t+1} by solving the following sub-problem

$$\mathbf{x}^{t+1} = \arg \min_{\mathbf{x} \in \mathbb{X}} r \cdot (f(\mathbf{x}^t) + \langle \nabla f(\mathbf{x}^t), \mathbf{x} - \mathbf{x}^t \rangle) + D_\phi(\mathbf{x}, \mathbf{x}^t). \quad (3.3)$$

Below we give two special versions of the MD method, each for a specific ϕ .

Example 3.3 (Projected gradient descent). When $\phi(\mathbf{x}) = \frac{1}{2} \|\mathbf{x}\|_2^2$, we have $D_\phi(\mathbf{x}, \mathbf{x}') = \|\mathbf{x} - \mathbf{x}'\|_2^2$, i.e., the

squared Euclidean distance. The MD method is reduced to the projected gradient descent (PGD) algorithm.

Example 3.4 (Entropic descent). When $\phi(\mathbf{x}) = \langle \mathbf{x}, \log \mathbf{x} \rangle$ and $\mathbb{X} = \{\mathbf{x} \geq \mathbf{0} : \mathbf{1}^\top \mathbf{x} = 1\}$, a probability simplex, we have $D_\phi(\mathbf{x}, \mathbf{x}') = \langle \mathbf{x}, \log \mathbf{x} - \log \mathbf{x}' \rangle$, known as the Kullback–Leibler (KL) divergence. The resulting algorithm is often referred to as the entropic descent (ED) algorithm. The sub-problem (3.3) of the ED method admits a simple analytic solution (Beck and Teboulle, 2003), which reads

$$x_k^{t+1} = \frac{x_k^t \cdot \exp(-r \cdot \nabla f(\mathbf{x}^t))}{\sum_{k=1}^n x_k^t \cdot \exp(-r \cdot \nabla f(\mathbf{x}^t))}. \quad (3.4)$$

4 Problem Formulation

We are now ready to describe the bilevel formulation for SCG. Since we are motivated mostly by transportation management problems, the narrative will be placed in that context hereafter. Accordingly, the leader in the SCG will be referred to as the transportation manager (the manager in short) and followers as travelers. Also, the lower level problem becomes a routing game played by travelers on a road network (referred to as the network hereafter). The network is modeled as a directed graph $\mathcal{G}(\mathbb{N}, \mathbb{A})$, where \mathbb{N} and \mathbb{A} are the set of nodes and links, respectively. Let $\mathbb{W} \subseteq \mathbb{N} \times \mathbb{N}$ be the set of origin-destination (OD) pairs and $\mathbb{K} \subseteq 2^{\mathbb{A}}$ be the set of available paths connecting all of the OD pairs. We use $\mathbb{K}_w \subseteq \mathbb{K}$ to denote the set of paths connecting $w \in \mathbb{W}$ and $\mathbb{A}_k \subseteq \mathbb{A}$ the set of all links on path $k \in \mathbb{K}$. Also, denote $\Sigma_{w,k}$ as the OD-path incidence with $\Sigma_{w,k} = 1$ if the path $k \in \mathbb{K}_w$ and 0 otherwise; and $\Lambda_{a,k}$ as the link-path incidence, with $\Lambda_{a,k} = 1$ if $a \in \mathbb{A}_k$ and 0 otherwise. For notational convenience, we write $\mathbf{\Lambda} = (\Lambda_{a,k})_{a \in \mathbb{A}, k \in \mathbb{K}}$ and $\mathbf{\Sigma} = (\Sigma_{w,k})_{w \in \mathbb{W}, k \in \mathbb{K}}$.

4.1 Lower Level: Routing Game

Let $\mathbf{d} = (d_w)_{w \in \mathbb{W}}$ be a vector with d_w denoting the number of travelers between $w \in \mathbb{W}$. The travelers' route choice is represented by a vector $\mathbf{p} = (p_k)_{k \in \mathbb{K}}$, where p_k equals the *proportion* of travelers selecting $k \in \mathbb{K}_w$. The feasible region for \mathbf{p} can be written as $\mathbb{P} = \{\mathbf{p} \geq \mathbf{0} : \mathbf{\Sigma} \mathbf{p} = \mathbf{1}\}$. Let $\mathbf{q} = (q_k)_{k \in \mathbb{K}}$ be a vector with $q_k = d_w$ if $k \in \mathbb{K}_w$, and $\mathbf{f} = (f_k)_{k \in \mathbb{K}}$ and $\mathbf{x} = (x_a)_{a \in \mathbb{A}}$, with f_k and x_a be the number of travelers using path k and link a , respectively. We have $\mathbf{q} = \mathbf{\Sigma}^\top \mathbf{d}$, $\mathbf{f} = \mathbf{q} \circ \mathbf{p}$, $\mathbf{\Sigma} \mathbf{f} = \mathbf{d}$ and $\mathbf{\Lambda} \mathbf{f} = \mathbf{x}$. We further define $\mathbf{u} = (u_a)_{a \in \mathbb{A}}$ as a vector of link cost, where u_a is determined by a continuous and strictly increasing function $u_a(x_a)$. Then, the vector of path cost $\mathbf{c} = \mathbf{\Lambda}^\top \mathbf{u}$. To summarize, the path cost function $c : \mathbb{P} \rightarrow \mathbb{R}^{|\mathbb{K}|}$ can be defined as

$$c(\mathbf{p}) = \mathbf{\Lambda}^\top \mathbf{u} = \mathbf{\Lambda}^\top u(\mathbf{\Lambda} \mathbf{f}) = \mathbf{\Lambda}^\top u(\mathbf{\Lambda} \mathbf{q} \circ \mathbf{p}). \quad (4.1)$$

We can now define WE as follows (Wardrop, 1952).

Definition 4.1 (Wardrop equilibrium). A route choice $\mathbf{p}^* \in \mathbb{P}$ is a WE if for all $w \in \mathbb{W}$ and $k \in \mathbb{K}_w$, we have $c_k(\mathbf{p}^*) > \min_{k' \in \mathbb{K}_w} c_{k'}(\mathbf{p}^*) \rightarrow p_k^* = 0$.

It is well known that WE defined above coincides with the solution to a variational inequality problem (VIP) (Dafermos, 1980).

Proposition 4.2 (VIP formulation for WE). A route choice $\mathbf{p}^* \in \mathbb{P}$ is a WE if and only if

$$\langle c(\mathbf{p}^*), \mathbf{p} - \mathbf{p}^* \rangle \geq 0, \quad \forall \mathbf{p} \in \mathbb{P}. \quad (4.2)$$

The following two propositions (Dafermos, 1980) characterize the geometry of \mathbb{P}^* .

Proposition 4.3. *If $c(\mathbf{p})$ is strongly monotone, then \mathbb{P}^* is a singleton.*

Proposition 4.4. *If $u(\mathbf{x})$ is strongly monotone, then $\mathbb{P}^* = \{\mathbf{p}^* \in \mathbb{P} : \Lambda \mathbf{q} \circ \mathbf{p}^* = \mathbf{x}^*\}$ is a polyhedron, where \mathbf{x}^* is the unique link flow at equilibrium.*

The assumption that $u(\mathbf{x})$ is strongly monotone is satisfied as long as $u_a(x_a)$ is strictly increasing with x_a , i.e., $u'_a(x_a) > 0$ for all $x_a \geq 0$. However, $c(\mathbf{p})$ is strongly monotone if and only if the Jacobian matrix $\nabla c(\mathbf{p}) = \Lambda^\top \nabla u(\mathbf{x}) \Lambda \text{diag}(\mathbf{q})$ is positively definite, which relies on stronger conditions. Specifically, a necessary and sufficient condition is that Λ has full column rank, which is rarely satisfied on networks of practical interests.

4.2 Upper Level: Optimization Problem

The manager's decision is denoted as a vector $\mathbf{z} \in \mathbb{Z} \subseteq \mathbb{R}^n$ (it means that \mathbf{z} is continuous rather than discrete), which may enter $u(\mathbf{x})$ either directly or indirectly, leading to a parameterized $u(\mathbf{x}; \mathbf{z})$, and hence $c(\mathbf{p}; \mathbf{z})$ as well as $\mathbb{P}^*(\mathbf{z})$. We assume the manager's cost be determined by a continuously differentiable function $l : \mathbb{P} \times \mathbb{Z} \rightarrow \mathbb{R}$. The manager's problem then reads

$$\begin{aligned} \min_{\mathbf{z} \in \mathbb{Z}, \mathbf{p}^* \in \mathbb{P}} \quad & l^*(\mathbf{z}) = l(\mathbf{p}^*; \mathbf{z}) \\ \text{s.t.} \quad & \mathbf{p}^* \in \mathbb{P}^*(\mathbf{z}). \end{aligned} \tag{4.3}$$

If the leader's cost is solely determined by the link flow and \mathbb{X}^* is a singleton (see Proposition 4.4), then any $\mathbf{p}^* \in \mathbb{P}^*(\mathbf{z})$ may be used to evaluate $l(\mathbf{p}^*; \mathbf{z})$. It is worth noting the condition stated in Proposition 4.4 may be violated in more general settings of the lower level problem. For example, when $u(\mathbf{x})$ is not separable (i.e., travel cost on a link may depend not only on the flow on that link but flows on other links), it is much harder to maintain strong monotonicity. In Section 8, we will show how the proposed approach can handle such more general problems with ease.

We close this section with a few classical examples of transportation management problems.

Example 4.5 (Second-best congestion pricing (Verhoef, 2002)). *To reduce traffic congestion, the manager may charge travelers a congestion toll on selected links, denoted as $\hat{\mathbb{A}} \subseteq \mathbb{A}$. Let $\mathbf{z} = (z_a)_{a \in \hat{\mathbb{A}}}$ be the toll on each link, the link cost function then can be written as $u(\mathbf{x}; \mathbf{z}) = u_{\text{time}}(\mathbf{x}) + \gamma \cdot \mathbf{z}$, where $u_{\text{time}}(\mathbf{x})$ is the time cost while γ is the time value of money. Under this setting, the feasible region of \mathbf{z} can be written as $\mathbb{Z} = \{\mathbf{z} \in \mathbb{R}_+^{|\hat{\mathbb{A}}|} : z_a = 0, \forall a \in \tilde{\mathbb{A}}\}$ and the cost of the manager is $l(\mathbf{p}^*; \mathbf{z}) = \langle \mathbf{x}^*, u_{\text{time}}(\mathbf{x}^*) \rangle$ ($\mathbf{x}^* = \Lambda \mathbf{q} \circ \mathbf{p}^*$), i.e., the total travel time of all travelers.*

Example 4.6 (Continues network design (Abdulaal and LeBlanc, 1979; Suwansirikul et al., 1987)). *This problem involves expanding road capacity on a predetermined set of links, denoted as $\tilde{\mathbb{A}} \subseteq \mathbb{A}$, to maximize congestion relief with a given budget. Let $\mathbf{v}_0 = (v_{0,a})_{a \in \mathbb{A}}$ be the original capacity of each link and $\mathbf{z} = (z_a)_{a \in \tilde{\mathbb{A}}}$ be the capacity added by the manager, the link cost function is then written as $u(\mathbf{x}; \mathbf{z}) = u_{\text{time}}(\mathbf{x}; \mathbf{v}_0 + \mathbf{z})$. Let $m : \mathbb{Z} \rightarrow \mathbb{R}$ be the cost associated with capacity enhancement. Given a budget m_0 , the feasible region of \mathbf{z} can be written as $\mathbb{Z} = \{\mathbf{z} \in \mathbb{R}_+^{|\tilde{\mathbb{A}}|} : m(\mathbf{z}) \leq m_0, z_a = 0, \forall a \in \hat{\mathbb{A}}\}$ and the cost of the manager is $l(\mathbf{p}^*; \mathbf{z}) = \langle \mathbf{x}^*, u_{\text{time}}(\mathbf{x}^*; \mathbf{v}_0 + \mathbf{z}) \rangle$, the total travel time. Alternatively, we may directly view the monetary budget as a soft constraint and assume that manager's cost is a weighted sum of a weighted sum of total travel time and monetary cost, namely $l(\mathbf{p}^*; \mathbf{z}) = \langle \mathbf{x}^*, u_{\text{time}}(\mathbf{x}^*; \mathbf{v}_0 + \mathbf{z}) \rangle + \beta \cdot m(\mathbf{z})$ for some $\beta > 0$.*

Example 4.7 (Stackelberg routing (Yang et al., 2007)). *In this problem, the manager attempts to minimize the total travel time by controlling the paths taken by a subset of travelers. Obviously, the advent of CAV technology has made such a scheme more viable than ever before. Let $\mathbf{z} = (z_k)_{k \in \mathbb{K}}$ be the route choice of the travelers under control (assuming they all use CAV) and \mathbf{d}_{av} be the corresponding demand. Similarly, we can define a vector $\mathbf{q}_{av} = (q_{av,k})_{k \in \mathbb{K}}$ with $q_{av,k} = d_{av,w}$ if $k \in \mathbb{K}_w$. The link cost function for the “free” travelers can be written as $u(\mathbf{x}; \mathbf{z}) = u_{time}(\mathbf{x} + \mathbf{x}_{av})$, where $\mathbf{x}_{av} = \mathbf{\Lambda} \text{diag}(\mathbf{q}_{av}) \mathbf{z}$ is the portion of link flow contributed by travelers using CAV. In this case, the feasible region of \mathbf{z} is $\mathbb{Z} = \{\mathbf{z} \geq \mathbf{0} : \mathbf{\Sigma} \mathbf{z} = \mathbf{1}\}$ and the cost of the manager is $l(\mathbf{p}^*; \mathbf{z}) = \langle \mathbf{x}^* + \mathbf{x}_{av}, u_{time}(\mathbf{x}^* + \mathbf{x}_{av}) \rangle$.*

5 Reformulation of the Routing Game

At the core of our approach to SCG is the reformulation of the routing game as a DiP. In this section, we propose a formulation based on ILD and give conditions under which it converges to a WE. In the literature, the stability of Nash (Wardrop) equilibrium under ILD is well known (Björnerstedt and Weibull, 1994; Sandholm, 2015). However, much less is known about its convergence to WE.

Let us first define a parameterized function $h : \mathbb{P} \times \mathbb{Z} \rightarrow \mathbb{P}$ such that

$$h_k(\mathbf{p}; \mathbf{z}) = \frac{p_k \cdot \exp(-r \cdot c_k(\mathbf{p}; \mathbf{z}))}{\sum_{k' \in \mathbb{K}_w} p_{k'} \cdot \exp(-r \cdot c_{k'}(\mathbf{p}; \mathbf{z}))}, \quad \forall k \in \mathbb{K}_w, \quad \forall w \in \mathbb{W}. \quad (5.1)$$

Starting from an initial solution $\mathbf{p}^0 \in \mathbb{P}$, ILD iteratively produces new solutions by $\mathbf{p}^{t+1} = h(\mathbf{p}^t; \mathbf{z})$ for some $r > 0$. It may be viewed as a variant of the logit choice model (McFadden, 1973; Ben-Akiva et al., 1985) in which the observed utility $(-r \cdot c_k(\mathbf{p}; \mathbf{z}))$ is scaled by the information content of the route choice probability $(\log(p_k))$.

5.1 Interpretation by Mirror Descent

We first note $\mathbf{p}_w^t = (p_k^t)_{k \in \mathbb{K}_w}$ can be viewed as the mixed strategy of a representative traveler from OD pair $w \in \mathbb{W}$ on day t (this interpretation was initially proposed in John Nash’s Ph.D. thesis). Assume each representative traveler aims to minimize their expected cost $\langle \mathbf{c}_w^t, \mathbf{p}_w^t \rangle$, where $\mathbf{c}_w^t = (c_k(\mathbf{p}^t; \mathbf{z}))_{k \in \mathbb{K}_w}$. Note that \mathbf{p}_w^t is the mixed strategy adopted by the representative traveler while \mathbf{p}^t is a vector of “stable” path choice probabilities. As the contribution of any traveler’s strategy to \mathbf{p}^t is negligible in a non-atomic game, \mathbf{c}_w^t is not affected by \mathbf{p}_w^t . Thus the derivative of the expected cost with respect to \mathbf{p}_w^t is simply \mathbf{c}_w^t .

To solve the representative traveler’s minimization problem, first recall the feasible set of their strategy as $\mathbb{P}_w = \{\mathbf{p}_w \geq \mathbf{0} : \mathbf{1}^\top \mathbf{p}_w = 1\}$. Applying the mirror descent method (see Section 3.2) yields

$$\mathbf{p}_w^{t+1} = \arg \min_{\mathbf{p}_w \in \mathbb{P}_w} r \cdot \langle \mathbf{c}_w^t, \mathbf{p}_w \rangle + D_{\phi_w}(\mathbf{p}_w, \mathbf{p}_w^t), \quad \forall w \in \mathbb{W}, \quad (5.2)$$

where $D_{\phi_w}(\mathbf{p}_w, \mathbf{p}_w^t)$ is the Bregman divergence induced by ϕ_w .

Proposition 5.1. *If $\phi_w(\mathbf{p}_w) = \langle \mathbf{p}_w, \log \mathbf{p}_w \rangle$, then the solution to the minimization problem (5.2) coincides with the ILD iterate $\mathbf{p}^{t+1} = h(\mathbf{p}^t; \mathbf{z})$ defined by Equation (5.1).*

Proposition 5.1 directly follows from Equation (3.4) in Example 3.4. It implies that ILD can be explained as the outcome of all travelers simultaneously minimizing their expected costs by a special mirror descent method.

Remark 5.2. This revelation helps connect ILD to classical traffic assignment algorithms, as well as DTD dynamical models. (1) *Frank-Wolfe (FW) algorithm*. If we set the KL divergence $D_{\phi_w}(\mathbf{p}_w, \mathbf{p}_w^t)$ in Equation (5.2) to zero, then ILD iterate is reduced to the solution to the sub-problem of the FW algorithm (Frank and Wolfe, 1956), a *standard* algorithm for finding WE in the transportation literature (LeBlanc et al., 1975; Florian and Nguyen, 1976). (2) *Euclidean projection (EP) method*. When $D_{\phi_w}(\mathbf{p}_w, \mathbf{p}_w^t)$ in Equation (5.2) is a squared Euclidean distance $\|\mathbf{p}_w - \mathbf{p}_w^t\|_2^2$, an ILD iterate equals a EP, the building block of projection algorithms for VIPs (Bertsekas and Gafni, 1982). (3) *Dual averaging (DA) method*. The MD method is also closely related to the dual averaging (also known as *online* MD) method (Nesterov, 2009). With the DA method, travelers aiming to minimize the expected cost will update their routing strategy on day k by changing the term $p_k \cdot \exp(-r \cdot c_k(\mathbf{p}; \mathbf{z}))$ in Equation 5.1 to $\exp(-r \cdot s_k^t)$,

$$p_k^t = \frac{\exp(-r \cdot s_k^t)}{\sum_{k' \in \mathbb{K}_w} \exp(-r \cdot s_{k'}^t)}, \quad \forall k \in \mathbb{K}_w, \quad \forall w \in \mathbb{W}, \quad (5.3)$$

where $s_k^0 = 0$ and $s_k^{t+1} = s_k^t + c_k(\mathbf{p}^t; \mathbf{z})$. (4) *DTD dynamical model*. The dual averaging method is conceptually similar to the DTD dynamical model of Watling (1999), which can be represented in the form of a DA iterate with $s_k^{t+1} = \alpha^t \cdot s_k^t + (1 - \alpha^t) \cdot c_k(\mathbf{p}^t; \mathbf{z})$ ($0 < \alpha^t < 1$).

5.2 Convergence Analysis

Before presenting the main convergence result, let us first define the *cover* of a path choice strategy $\mathbf{p}_w \in \mathbb{P}_w$, denoted by $\mathbb{Q}_w(\mathbf{p}_w) \subseteq \mathbb{P}_w$, as

$$\mathbb{Q}_w(\mathbf{p}_w) = \{\mathbf{p}'_w \in \mathbb{P}_w : \text{supp}(\mathbf{p}'_w) \subseteq \text{supp}(\mathbf{p}_w)\}.$$

Accordingly, the cover of $\mathbf{p} \in \mathbb{P}$ is defined as $\mathbb{Q}(\mathbf{p}) = \prod_{w \in \mathbb{W}} \mathbb{Q}_w(\mathbf{p}_w)$. If $\mathbf{p}' \in \mathbb{Q}(\mathbf{p})$, we say \mathbf{p}' is *covered* by \mathbf{p} , which means any path with positive choice probability in \mathbf{p}' must also have positive choice probability in \mathbf{p} , but not vice versa. The following lemma (Kullback, 1997) characterizes the property of the KL divergence, which is central to the ILD scheme (see Proposition 5.1).

Lemma 5.3. *For any $\mathbf{p}_w, \mathbf{p}'_w \in \mathbb{P}_w$, $D_{\phi_w}(\mathbf{p}_w, \mathbf{p}'_w) < \infty$ if and only if \mathbf{p}'_w is covered by \mathbf{p}_w .*

The next result reformulates the ILD iterate as a VIP.

Lemma 5.4. *For any $\mathbf{p}^t \in \mathbb{P}$, $\mathbf{p}^{t+1} = h(\mathbf{p}^t; \mathbf{z})$ if and only if for all $w \in \mathbb{W}$,*

$$\langle r \cdot c_w(\mathbf{p}^t; \mathbf{z}) + \nabla \phi_w(\mathbf{p}_w^{t+1}) - \nabla \phi_w(\mathbf{p}_w^t), \mathbf{p}_w - \mathbf{p}_w^{t+1} \rangle \geq 0, \quad \forall \mathbf{p}_w \in \mathbb{Q}_w(\mathbf{p}_w^t). \quad (5.4)$$

Sketch of proof. Proposition 5.1 first implies that $\mathbf{p}^{t+1} = h(\mathbf{p}^t; \mathbf{z})$ if and only if \mathbf{p}_w^{t+1} is defined by Equation (5.2) — a convex program. Lemma 5.4 then follows from the well-known equivalence between a convex program and a VIP (Kinderlehrer and Stampacchia, 2000). In the resulting VIP formulation (5.4), we require any feasible solution \mathbf{p}_w be covered by \mathbf{p}_w^t because only then the objective function in (5.2) is finite, and thus well-defined (see Lemma 5.3). We refer the readers to Appendix A.1 for detailed proof. \square

We next examine the relation between a WE and a fixed point of the ILD.

Lemma 5.5. *If $\mathbf{p}^* \in \mathbb{P}^*(\mathbf{z})$, then $\mathbf{p}^* = h(\mathbf{p}^*; \mathbf{z})$. Conversely, if $\hat{\mathbf{p}} = h(\hat{\mathbf{p}}; \mathbf{z})$ and there exists some $\mathbf{p}^* \in \mathbb{P}^*(\mathbf{z})$ such that $\mathbf{p}^* \in \mathbb{Q}(\hat{\mathbf{p}})$, then $\hat{\mathbf{p}} \in \mathbb{P}^*(\mathbf{z})$.*

Sketch of proof. We first note any $\mathbf{p}^* \in \mathbb{P}^*(\mathbf{z})$ must itself be a fixed point of ILD iterations. Applying Lemma 5.4, this means

$$\langle c(\mathbf{p}^*; \mathbf{z}), \mathbf{p} - \mathbf{p}^* \rangle \geq 0, \quad \forall \mathbf{p} \in \mathbb{Q}(\mathbf{p}^*). \quad (5.5)$$

VIP (5.5) must hold because $\mathbf{p}^* \in \mathbb{P}^*(\mathbf{z})$ implies $\langle c(\mathbf{p}^*; \mathbf{z}), \mathbf{p} - \mathbf{p}^* \rangle \geq 0$ for all $\mathbf{p} \in \mathbb{P}$, where $\mathbb{Q}(\mathbf{p}^*) \subseteq \mathbb{P}$. The reverse statement, that a fixed point of ILD iterates must be a WE, does not hold in general. It requires there to exist at least one equilibrium strategy covered by the fixed point. We refer the readers to Appendix A.2 for more details. \square

We are now ready to condition the initial point \mathbf{p}^0 for the convergence of ILD iterates to a WE. First, note $\mathbf{p}^t \in \mathbb{Q}(\mathbf{p}^0)$ for all $t \geq 0$, i.e., a strategy not covered by the initial strategy can never be reached by ILD iterates alone. This property derives from the information content term in Equation (5.1), and it means, under ILD, travelers will consider *only* the paths initially included in the choice set as they update their strategies. It follows \mathbf{p}^t would never converge to a WE if the intersection of $\mathbb{Q}(\mathbf{p}^0)$ and $\mathbb{P}^*(\mathbf{z})$ is empty. Thus, to ensure convergence, $\mathbb{Q}(\mathbf{p}^0) \cap \mathbb{P}^*(\mathbf{z})$ must be nonempty. Such a condition can always be achieved by expanding $\text{supp}(\mathbf{p}^0)$. Our main result (Theorem 5.7) will further verify that this necessary condition is also sufficient, i.e., whenever there exists $\mathbf{p}^* \in \mathbb{P}^*(\mathbf{z})$ with $\mathbf{p}^* \in \mathbb{Q}(\mathbf{p}^0)$, \mathbf{p}^t would converge to an equilibrium, as long as the learning rate r is properly tuned. To tune the learning rate r , we first recall Proposition 2.1 in Marcotte and Wu (1995), restated as Lemma 5.6 below.

Lemma 5.6. *Suppose $c(\cdot; \mathbf{z})$ be twice continuously differentiable, L_z -Lipschitz continuous and monotone on \mathbb{P} . If $\|\nabla_{\mathbf{p}} c(\mathbf{p}; \mathbf{z}) - \nabla_{\mathbf{p}} c(\mathbf{p}; \mathbf{z})^\top\|_2 \leq \|\nabla_{\mathbf{p}} c(\mathbf{p}; \mathbf{z}) + \nabla_{\mathbf{p}} c(\mathbf{p}; \mathbf{z})^\top\|_2$ (plainly, this may be interpreted as $\nabla_{\mathbf{p}} c(\mathbf{p}; \mathbf{z})$ being not “too asymmetric”) for all $\mathbf{p} \in \mathbb{P}$, then $c(\cdot; \mathbf{z})$ is c_z -cocoercive ($c_z = 1/4L_z$) on \mathbb{P} , i.e., for all $\mathbf{p}, \mathbf{p}' \in \mathbb{P}$,*

$$\langle c(\mathbf{p}'; \mathbf{z}) - c(\mathbf{p}; \mathbf{z}), \mathbf{p}' - \mathbf{p} \rangle \geq c_z \cdot \|c(\mathbf{p}'; \mathbf{z}) - c(\mathbf{p}; \mathbf{z})\|_2^2. \quad (5.6)$$

For the routing game defined in Section 4.1, its path cost function $c(\mathbf{p}; \mathbf{z})$ (i) is L_z -Lipschitz continuous because \mathbb{P} is compact; (ii) is monotone because $u(\mathbf{x}; \mathbf{z})$ is monotone; and (iii) has a symmetric Jacobian matrix $\nabla_{\mathbf{p}} c(\mathbf{p}; \mathbf{z})$ because $u(\mathbf{x}; \mathbf{z})$ is separable. Thus, $c(\mathbf{p}; \mathbf{z})$ in our setting is c_z -cocoercive. Our main convergence result, given below, builds on the cocoercivity of $c(\cdot; \mathbf{z})$.

Theorem 5.7. *Suppose $c(\cdot; \mathbf{z})$ is c_z -cocoercive on \mathbb{P} . If $r < 2c_z$ and $\mathbb{Q}(\mathbf{p}^0) \cap \mathbb{P}^*(\mathbf{z})$ is nonempty, then the sequence $\{\mathbf{p}^t\}$ defined by ILD iterate (5.1) converges to $\mathbb{P}^*(\mathbf{z})$.*

Sketch of proof. For any $\mathbf{p}, \mathbf{p}' \in \mathbb{P}$, we define $\tilde{D}_\phi(\mathbf{p}, \mathbf{p}') = \sum_{w \in \mathbb{W}} D_{\phi_w}(\mathbf{p}_w, \mathbf{p}'_w)$ to measure the “distance” between \mathbf{p} and \mathbf{p}' . Our goal is to prove there exists $\mathbf{p}^* \in \mathbb{P}^*(\mathbf{z})$ such that $\tilde{D}_\phi(\mathbf{p}^*, \mathbf{p}^t)$ decreases to 0 when $t \rightarrow \infty$. Given $c(\cdot; \mathbf{z})$ is c_z -cocoercive, we can show, for all $\mathbf{p}^* \in \mathbb{P}^*(\mathbf{z})$,

$$\tilde{D}_\phi(\mathbf{p}^*, \mathbf{p}^t) - \tilde{D}_\phi(\mathbf{p}^*, \mathbf{p}^{t+1}) \geq \frac{2c_z - r}{4c_z} \cdot \|\mathbf{p}^t - \mathbf{p}^{t+1}\|_2^2. \quad (5.7)$$

For a \mathbf{p}^* covered by \mathbf{p}^0 per the initial condition, $\tilde{D}_\phi(\mathbf{p}^*, \mathbf{p}^0) < \infty$ per Lemma 5.3. For such \mathbf{p}^* , the divergence $\tilde{D}_\phi(\mathbf{p}^*, \mathbf{p}^t)$ is monotonically decreasing as long as $r < 2c_z$ according to Equation (5.7). Thus, the limit of $\tilde{D}_\phi(\mathbf{p}^*, \mathbf{p}^t)$ exists according to the monotone convergence theorem. Letting $t \rightarrow \infty$ on both sides of Equation (5.7), the squeeze theorem implies $\|\mathbf{p}^t - \mathbf{p}^{t+1}\|_2$ converges to 0. Furthermore, since \mathbb{P} is compact,

the Bolzano–Weierstrass theorem guarantees the sequence $\{p^t\}$ must have a convergent subsequence $\{p^{t_j}\}$. Using the conditions that $\|p^{t_{j+1}} - p^{t_j}\|_2 \rightarrow 0$ and $h(\cdot; z)$ is continuous, we then prove the limit of the subsequence, denoted as \hat{p} , satisfies $\hat{p} = h(\hat{p}; z)$. We next claim $p^* \in \mathbb{Q}(p^0)$ implies $p^* \in \mathbb{Q}(\hat{p})$. Otherwise, $D_\phi(p^*, \hat{p})$ would be unbounded, which is impossible given $D_\phi(p^*, p^t)$ is monotonically decreasing. This allows us to invoke Lemma 5.5 to show the limit \hat{p} is indeed a WE. Hence, $\tilde{D}_\phi(\hat{p}, p^t) \rightarrow 0$ when $t \rightarrow \infty$, which concludes the proof. We refer the readers to Appendix A.3 for the full proof. \square

Theorem 5.7 resembles but extends Marcotte and Wu (1995)’s result for the projection method. It provides the theoretical guarantee for reformulating the WE of a routing game as the limit point of the ILD.

6 Routing Game as a Differentiable Program (DiP)

Having formulated the routing game as ILD and proven its convergence, we proceed in this section to represent it as a DiP. The representation allows us to evaluate the gradient of the manager’s objective with respect to their decisions using automatic differentiation (AD).

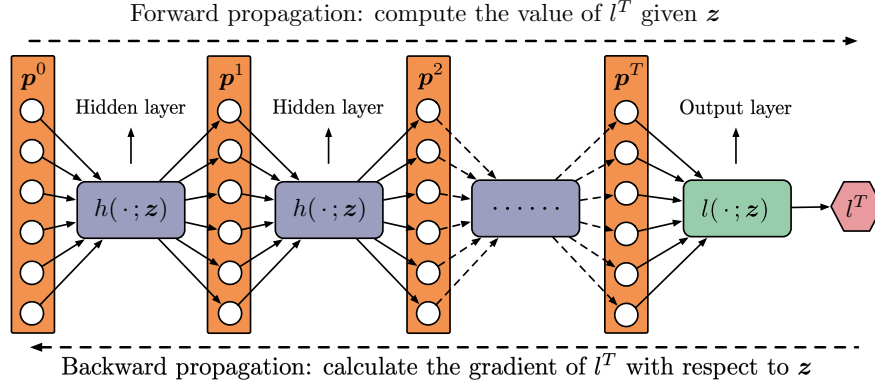


Figure 1: A representation of the manager’s cost in an SCG.

Recall that with ILD we can define the routing strategy on day t recursively as $h^{(t)}(p; z) = h(h^{(t-1)}(p; z); z)$. Thus, the manager’s cost on a given day, say T , can be *explicitly* expressed as $l^T = l(p^T; z)$, where $p^T = h^{(T)}(p^0; z)$. It can be viewed as the output of a DiP structured as in Figure 1. In the graph, $h(\cdot; z)$ represents the hidden layers and $l(\cdot; z)$ the output layer, to borrow the terminology from the deep learning community. In this “DNN”, the manager’s decision z is embedded as weights shared by all these layers. Then, calculating $\partial l^T / \partial z$ is reduced to computing the gradient of a DNN’s output with respect to its weights, a routine task in deep learning problems.

Algorithms 3 and 4 give overall structures of Forward Propagation (FP) and Backward Propagation (BP), respectively, when the routing game is formulated as ILD. We note again BP can be automatically programmed if one is inclined to take advantage of such tools as PyTorch and TensorFlow. The BP algorithm is presented here in order to demonstrate and highlight the scalability of AD in our problem.

Recall that $h(p; z) = q / \Sigma^\top \Sigma q$, where $q = \exp(-r \cdot c(p; z)) \circ p$ and $c(p; z) = \Lambda^\top u(\Lambda q \circ p; z)$. For the purpose of illustration, we specify $u(x; z)$ and $l(p; z)$ according to Example 4.5 in Section 4.2, and set the link travel time function $u_{\text{time}}(x) = a + b \circ x$. The pseudocode of FP and BP for this specific example is

Algorithm 3 The overall structure of FP.

```

1: for  $t = 0, \dots, T - 1$  do
2:    $\mathbf{p}^{t+1} = h(\mathbf{p}^t; \mathbf{z})$ 
3: end for
4:  $l^T = l(\mathbf{p}^T; \mathbf{z})$ 

```

Algorithm 4 The overall structure of BP.

```

1:  $\bar{\mathbf{p}}^T = \nabla_{\mathbf{p}} l(\mathbf{p}^T; \mathbf{z})$  and  $\bar{\mathbf{z}} = \nabla_{\mathbf{z}} l(\mathbf{p}^T; \mathbf{z})$ 
2: for  $t = T - 1, \dots, 0$  do
3:    $\bar{\mathbf{p}}^t = \nabla_{\mathbf{p}} h(\mathbf{p}^t; \mathbf{z}) \bar{\mathbf{p}}^{t+1}$  and  $\bar{\mathbf{z}} += \nabla_{\mathbf{z}} h(\mathbf{p}^t; \mathbf{z}) \bar{\mathbf{p}}^{t+1}$ 
4: end for

```

given in Algorithms 5 and 6. To help the reader understand the code, take line 6 for example. By applying the chain rule to this line in Algorithm 5, we have

$$\bar{\mathbf{c}}^t = \frac{\partial l^T}{\partial \mathbf{c}^t} = \frac{\partial \mathbf{e}^t}{\partial \mathbf{c}^t} \cdot \frac{\partial l^T}{\partial \mathbf{e}^t} = -r \cdot \exp(-r \cdot \mathbf{c}^t) \circ \frac{\partial l^T}{\partial \mathbf{e}^t} = -r \cdot \mathbf{e}^t \circ \bar{\mathbf{e}}^t,$$

which corresponds to line 8 in Algorithm 6.

Algorithm 5 FP in Example 4.5

```

1: for  $t = 0, \dots, T - 1$  do
2:    $\mathbf{f}^t = \mathbf{q} \circ \mathbf{p}^t$  ▷  $|\mathbb{K}|$ 
3:    $\mathbf{x}^t = \mathbf{\Lambda} \mathbf{f}^t$  ▷  $\text{nnz}(\mathbf{\Lambda})$ 
4:    $\mathbf{u}^t = \mathbf{a} + \mathbf{b} \circ \mathbf{x}^t + \gamma \cdot \mathbf{z}$  ▷  $4|\mathbb{A}|$ 
5:    $\mathbf{c}^t = \mathbf{\Lambda}^\top \mathbf{u}^t$  ▷  $\text{nnz}(\mathbf{\Lambda})$ 
6:    $\mathbf{e}^t = \exp(-r \cdot \mathbf{c}^t)$  ▷  $2|\mathbb{K}|$ 
7:    $\mathbf{g}^t = \mathbf{e}^t \circ \mathbf{p}^t$  ▷  $|\mathbb{K}|$ 
8:    $\mathbf{s}^t = \mathbf{\Sigma}^\top \mathbf{\Sigma} \mathbf{g}^t$  ▷  $2\text{nnz}(\mathbf{\Sigma})$ 
9:    $\mathbf{p}^{t+1} = \mathbf{g}^t / \mathbf{s}^t$  ▷  $|\mathbb{K}|$ 
10: end for
11:  $\mathbf{f}^T = \mathbf{q} \circ \mathbf{p}^T$  ▷  $|\mathbb{K}|$ 
12:  $\mathbf{x}^T = \mathbf{\Lambda} \mathbf{f}^T$  ▷  $\text{nnz}(\mathbf{\Lambda})$ 
13:  $l^T = \langle \mathbf{a} + \mathbf{b} \circ \mathbf{x}^T, \mathbf{x}^T \rangle$  ▷  $3|\mathbb{A}|$ 

```

Algorithm 6 BP in Example 4.5

```

1:  $\bar{\mathbf{x}}^T = \mathbf{a} + 2\mathbf{b} \circ \mathbf{x}^T$  ▷  $3|\mathbb{A}|$ 
2:  $\bar{\mathbf{f}}^T = \mathbf{\Lambda}^\top \bar{\mathbf{x}}^T$  ▷  $\text{nnz}(\mathbf{\Lambda})$ 
3:  $\bar{\mathbf{p}}^T = \mathbf{q} \circ \bar{\mathbf{f}}^T$  ▷  $|\mathbb{K}|$ 
4: for  $t = T - 1, \dots, 0$  do
5:    $\bar{\mathbf{g}}^t = \bar{\mathbf{p}}^{t+1} / \mathbf{s}^t$  and  $\bar{\mathbf{s}}^t = -\bar{\mathbf{p}}^{t+1} / (\mathbf{s}^t)^2$  ▷  $3|\mathbb{K}|$ 
6:    $\bar{\mathbf{g}}^t = \mathbf{\Sigma}^\top \mathbf{\Sigma} \bar{\mathbf{s}}^t$  ▷  $2\text{nnz}(\mathbf{\Sigma})$ 
7:    $\bar{\mathbf{p}}^t = \mathbf{e}^t \circ \bar{\mathbf{g}}^t$  and  $\bar{\mathbf{e}}^t = \mathbf{p}^t \circ \bar{\mathbf{g}}^t$  ▷  $2|\mathbb{K}|$ 
8:    $\bar{\mathbf{c}}^t = -r \cdot \mathbf{e}^t \circ \bar{\mathbf{e}}^t$  ▷  $2|\mathbb{K}|$ 
9:    $\bar{\mathbf{u}}^t = \mathbf{\Lambda} \bar{\mathbf{c}}^t$  ▷  $\text{nnz}(\mathbf{\Lambda})$ 
10:   $\bar{\mathbf{x}}^t = \mathbf{b} \circ \bar{\mathbf{u}}^t$  and  $\bar{\mathbf{z}} = \gamma \cdot \bar{\mathbf{u}}^t$  ▷  $2|\mathbb{A}|$ 
11:   $\bar{\mathbf{f}}^t = \mathbf{\Lambda}^\top \bar{\mathbf{x}}^t$  ▷  $\text{nnz}(\mathbf{\Lambda})$ 
12:   $\bar{\mathbf{p}}^t += \mathbf{q} \circ \bar{\mathbf{f}}^t$  ▷  $|\mathbb{K}|$ 
13: end for

```

Note that only two types of basic operations are involved in both phases. (1) Element-wise vector operations (e.g., multiplication, division, and exponentiation); the complexity of these operations is determined by the size of the vector. (2) Multiplication between a 0-1 sparse matrix and a vector; its complexity is determined by the number of nonzero elements in the sparse matrix. For example, the OD-path incidence matrix $\mathbf{\Sigma}$ is a sparse matrix with only one nonzero element in each column. Thus, $\text{nnz}(\mathbf{\Sigma}) = |\mathbb{K}|$. As for the link-path incidence matrix $\mathbf{\Lambda}$, the number of nonzero elements $\text{nnz}(\mathbf{\Lambda}) = \bar{N}_{\text{link}} \cdot |\mathbb{K}|$, where \bar{N}_{link} is the average number of links in a path. In the pseudocode, the complexity of each operation is given at the end of the line.

Let us denote N_{forward} and N_{backward} as the complexities of Algorithms 3 and 4, respectively. We then obtain

$$\begin{aligned}
N_{\text{forward}} &= (7T + 1) \cdot |\mathbb{K}| + (4T + 3) \cdot |\mathbb{A}| + (2T + 1) \cdot \bar{N}_{\text{link}} \cdot |\mathbb{K}|; \\
N_{\text{backward}} &= (10T + 1) \cdot |\mathbb{K}| + (2T + 3) \cdot |\mathbb{A}| + (2T + 1) \cdot \bar{N}_{\text{link}} \cdot |\mathbb{K}|.
\end{aligned}$$

We can now compare the complexities. Note that we shall ignore all operations only related to $|\mathbb{A}|$, since $|\mathbb{A}| \ll |\mathbb{K}|$. The ratio between N_{forward} and N_{backward} for Examples 4.5 can be estimated as

$$(2T \cdot \bar{N}_{\text{link}} + \bar{N}_{\text{link}} + 10T + 1) / (2T \cdot \bar{N}_{\text{link}} + \bar{N}_{\text{link}} + 7T + 1),$$

where $T \geq 0$ and $\bar{N}_{\text{link}} \geq 1$. It can be easily verified that the ratio is upper bounded by $(2+10)/(2+7) = 4/3$. When $T \cdot \bar{N}_{\text{link}}$ is sufficiently large, the ratio would be close to 1.

Although these results are obtained for a specific SCG (Example 4.5), they can be generalized to a wide range of SCG settings (including Examples 4.6 and 4.7). Indeed, these SCGs mainly differ in how the manager's decision affects the link cost received by the travelers, i.e., how the function $u(\mathbf{x}; \mathbf{z})$ is defined. Yet, the calculation in both FP and BP associated with $u(\mathbf{x}; \mathbf{z})$ scale with $|\mathbb{A}| \ll |\mathbb{K}|$, which can be safely ignored for our purpose (in Example 4.7, we may equivalently view $\mathbf{x}_{\text{av}} = \mathbf{\Lambda} \text{diag}(\mathbf{q}_{\text{av}}) \mathbf{z}$ as the decision variable to satisfy this statement).

To summarize, we have shown (i) the complexity of differentiating the manager's cost on day T is dominated by the term $T \cdot \bar{N}_{\text{link}} \cdot |\mathbb{K}|$; and (ii) the number of arithmetic operations required in backward propagation is tightly bounded by that in forward propagation.

Remark 6.1 (Alternative DiP reformations). Can we recast the routing game by any iterative process that provably converges to a WE? One idea that immediately comes to mind is the Frank-Wolfe algorithm. Could we treat the Frank-Wolfe iterates as a DiP? We believe the answer is negative, because each iteration of the algorithm gets a descent direction by solving a linear program (LP), whose optimal solution may not be smooth. In contrast, an EP iterate is almost everywhere differentiable (Rademacher, 1919). However, because it does not admit an analytical solution, carrying out FP/BP over the DiP resulted from EP is not particularly efficient for EP (Amos and Kolter, 2017). Finally, most logit-based DTD dynamical processes are differentiable, and they would behave similarly to ILD, provided their convergence to a WE can be established.

7 Algorithms for Stackelberg Congestion Games

In this section, we devise two algorithms for SCGs, built on the results developed in the previous sections. By replacing the equilibrium constraint $\mathbf{p}^* \in \mathbb{P}^*(\mathbf{z})$ in the original formulation (4.3) by its DiP counterpart, we obtain the following formulation:

$$\begin{aligned} \min_{\mathbf{z} \in \mathbb{Z}} \quad & l(\mathbf{p}^*; \mathbf{z}), \\ \text{s.t.} \quad & \mathbf{p}^* = \lim_{T \rightarrow \infty} h^{(T)}(\mathbf{p}^0; \mathbf{z}), \end{aligned} \tag{7.1}$$

where $\mathbf{p}^0 \in \mathbb{P}$ is the travelers' initial routing strategy. The new formulation is easier to solve than the original (4.3) for the following two reasons:

1. It bypasses the problem of “choosing” an equilibrium when there could be many. The equilibrium selected is the limit of the evolutionary dynamics, which is interpreted as an outcome corresponding to a specific choice behavior. The two formulations (4.3) and (7.1) are equivalent if the link flow at equilibrium is unique and the manager's objective function is solely determined by the link flow. However, the latter will come in handy in more general settings, as we shall show in Section 8.
2. The objective function of the new formulation (7.1) is differentiable under much weaker conditions. Notably, its differentiability does not require the uniqueness of the lower-level equilibrium problem, a requirement for performing implicit differentiation. In addition, the gradient can also be computed with ease using AD, as discussed in Section 6.

To simplify the presentation, we introduce a few more assumptions.

Assumption 7.1. Both $l(\mathbf{p}; \mathbf{z})$ and $u(\mathbf{x}; \mathbf{z})$ are continuously differentiable.

Assumption 7.2. The constraint set of the manager’s decisions, \mathbb{Z} , is convex.

Assumption 7.3. There exists $r > 0$ such that $r < \inf_{\mathbf{z} \in \mathbb{Z}} 1/2L_{\mathbf{z}}$.

Assumption 7.4. The initial strategy $\mathbf{p}^0 > 0$.

Among other things, Assumptions 7.3 and 7.4 ensure the convergence of the ILD iterates $h^{(t)}(\mathbf{p}; \mathbf{z})$ towards $\mathbb{P}^*(\mathbf{z})$ when $t \rightarrow \infty$. Importantly, we may “truncate” the iterates at a T large enough to ensure $\mathbf{p}^T = h^{(T)}(\mathbf{p}^0; \mathbf{z})$ be sufficiently close to $\mathbb{P}^*(\mathbf{z})$. With this approximation, we may minimize $l(\mathbf{p}^T; \mathbf{z})$ rather than $l(\mathbf{p}^*; \mathbf{z})$. Assumption 7.1 guarantees the differentiability of $l(\mathbf{p}^T; \mathbf{z})$; Assumption 7.2 enables the use of most first-order methods to minimize $l^{(T)}(\mathbf{p}; \mathbf{z})$.

Remark 7.5 (Relaxation of the assumptions). Some of these assumptions may be relaxed should an application call for it. (i) When \mathbb{Z} is non-convex, it may be turned into penalty terms in the objective function to satisfy Assumption 7.2. (ii) The learning rate r can be adjusted according to \mathbf{z} to be smaller than $1/2L_{\mathbf{z}}$. (iii) Although requiring $\mathbf{p}^0 > 0$ seems rather strong (given the potential size of \mathbb{K}), we note the support of \mathbf{p}^0 only needs to cover the paths used at an equilibrium $\mathbf{p}^* \in \mathbb{P}^*(\mathbf{z})$ for a given \mathbf{z} . The challenge, of course, is that for any \mathbf{z} , one would not know precisely which set can cover all equilibrium paths until the equilibrium is reached. This challenge may be tackled in two ways in practice. First, a column generation procedure can be employed to dynamically expand the set with new paths identified as having the potential to be used at equilibrium. This approach requires \mathbb{K} to be constructed from scratch each time the routing game is solved as a subroutine of the bilevel program. Another possibility is to predetermine \mathbb{K} , once and for all before the bilevel program is solved. This may be achieved by solving the routing game multiple times, using algorithms designed to find all UE path flows (Xie et al., 2018; Feng et al., 2020). A different set of upper-level design variables is fed into the routing game each time, and the union of the UE paths obtained from all scenarios then provides an estimate for \mathbb{K} .

7.1 A Double-Loop Mirror Descent Algorithm

For all $\mathbf{z} \in \mathbb{Z}$, Assumptions 7.3 and 7.4 guarantee that $\mathbf{p}^T = h^{(T)}(\mathbf{p}^0; \mathbf{z})$ can be arbitrarily close to $\mathbb{P}^*(\mathbf{z})$ for sufficiently large T . In the algorithm, we need a gap function $\delta : \mathbb{P} \times \mathbb{Z} \rightarrow \mathbb{R}$ that measures the distance between any $\mathbf{p} \in \mathbb{P}$ and $\mathbb{P}^*(\mathbf{z})$. A widely-used measure is $\delta(\mathbf{p}; \mathbf{z}) = -\langle c(\mathbf{p}; \mathbf{z}), \mathbf{p}' - \mathbf{p} \rangle$, where $\mathbf{p}' \in \arg \min_{\mathbf{p}'' \in \mathbb{P}} \langle c(\mathbf{p}; \mathbf{z}), \mathbf{p}'' \rangle$ (known as the all-or-nothing assignment in the traffic assignment literature). We may add the gap measure into (7.1), which yields

$$\begin{aligned} \min_{\mathbf{z} \in \mathbb{Z}} \quad & l(\mathbf{p}^T; \mathbf{z}), \\ \text{s.t.} \quad & \mathbf{p}^T = h^{(T)}(\mathbf{p}^0; \mathbf{z}), \\ & T \text{ is sufficiently large so that } \delta(\mathbf{p}^T; \mathbf{z}) \leq \epsilon, \end{aligned} \tag{7.2}$$

where ϵ is a predetermined convergence threshold. By adjusting ϵ , Problem (7.2) can be made arbitrarily close to Problem (7.1). We next devise a mirror descent (MD) method for Problem (7.2). We begin with the choice of a Bregman divergence $D_\psi : \mathbb{Z} \times \mathbb{Z} \rightarrow \mathbb{R}$ that is application specific. For example, our experience indicates the squared Euclidean distance is suitable for Examples 4.5 and Example 4.6 and the KL divergence works better in Example 4.7. Algorithm 7 gives the pseudocode. The manager first anticipates the evolutionary

Algorithm 7 A Double-Loop MD (Dol-MD) algorithm for solving Problem (7.2).

```

1: Input:  $\mathbf{p}^0 \in \mathbb{P}$ ,  $\mathbf{z}^0 \in \mathbb{Z}$ , upper-level learning rate  $\rho$ , lower-level learning rate  $r$ 
2: for  $i = 0, 1, \dots$  do
3:   FP (running Algorithm 3 until convergence):
4:   for  $t = 0, 1, \dots$  do
5:     Run  $\mathbf{p}^{t+1} = h(\mathbf{p}^t; \mathbf{z}^i)$ .
6:     If  $\delta(\mathbf{p}^t; \mathbf{z}^i) \leq \epsilon$ , break and set  $T = t$  and  $\mathbf{l}^T = l(\mathbf{p}^T; \mathbf{z})$ .
7:   end for
8:   BP: Calculate  $\mathbf{l}_z = \partial l^T / \partial \mathbf{z}_i$  by calling Algorithm 4 (implemented via AD).
9:   Update the manager's decision: set  $\mathbf{z}^{i+1} = \arg \min_{\mathbf{z} \in \mathbb{Z}} \rho \cdot \langle \mathbf{l}_z, \mathbf{z} - \mathbf{z}^i \rangle + D_\psi(\mathbf{z}, \mathbf{z}^i)$ .
10:  If  $\mathbf{z}^i$  converges, break and set  $\mathbf{z}^* = \mathbf{z}^i$  and  $\mathbf{p}^* = \mathbf{p}^T$ ;
11: end for

```

process until the equilibrium is achieved (i.e., when the gap becomes sufficiently small). In Algorithm 7, this is described as forward propagation (FP). The process is rather similar to Algorithm 3, except here the total number of iterations T is not predetermined but set based on the gap. Then, Algorithm 4 is called to evaluate the gradient backward over the computational graph built in FP. As shown in the previous section, the complexity of calculating \mathbf{l}_z (hence its gradient) scales linearly with T . Thus, if a large number of iterations is required in FP, the computational efficiency may be compromised, because, among other things, building a computational graph large enough to store all the iterations for backward propagation (BP) can be memory intensive. This observation motivates us to explore ways that restrict T , leading to a more efficient algorithm presented in the next section.

7.2 A Single-Loop Mirror Descent Algorithm

Algorithm 7 contains a double loop that is standard in dealing with bilevel programs: the inner loop (over t) seeks equilibrium whereas the outer loop (over i) optimizes the manager's decision. As mentioned in Section 2.3, the toll on the computational overhead imposed by such a double-loop structure has prompted many to invent single-loop heuristics. Of these, the most widely tested is to approximate the Stackelberg game with the following Cournot game (Fisk, 1984),

$$\tilde{\mathbf{z}} \in \arg \min_{\mathbf{z} \in \mathbb{Z}} l(\tilde{\mathbf{p}}; \tilde{\mathbf{z}}), \quad \text{and} \quad \tilde{\mathbf{p}} \in \mathbb{P}^*(\tilde{\mathbf{z}}). \quad (7.3)$$

This approximation scheme is not applicable when the manager's cost is solely determined by the travelers' strategy $\tilde{\mathbf{p}}$ (i.e., independent of \mathbf{z} , cf. Example 4.5).

We set out to further develop the above scheme by adding two new features: co-evolution and limited anticipation. This results in a new single-loop MD algorithm (dubbed SiL-MD) whose solution quality can be properly controlled. By limited anticipation, we mean the manager would not completely give up anticipating travelers' response as in (7.3), where the manager's objective function $l(\tilde{\mathbf{p}}; \tilde{\mathbf{z}})$ implies $\tilde{\mathbf{p}}$ (the *current* equilibrium solution) are taken as a *fixed* input to update their decision in each iteration. When limited anticipation is allowed, (7.5) is turned into

$$\tilde{\mathbf{z}} \in \arg \min_{\mathbf{z} \in \mathbb{Z}} l^{(T)}(\tilde{\mathbf{p}}; \tilde{\mathbf{z}}), \quad \text{and} \quad \tilde{\mathbf{p}} \in \mathbb{P}^*(\tilde{\mathbf{z}}). \quad (7.4)$$

Here the objective function $l^{(T)}(\tilde{\mathbf{p}}; \tilde{\mathbf{z}})$ means the manager will look ahead T steps along the travelers' evolutionary path. More specifically, we have $l^{(T)}(\mathbf{p}; \mathbf{z}) = l(h^{(T)}(\mathbf{p}; \mathbf{z}); \mathbf{z})$ with $h^{(T)}$ being the T th ILD iterate, starting from \mathbf{p} . Clearly, when $T = 0$, (7.4) is reduced to (7.3). Also clear is the fact that one can always find a T large enough to ensure (7.4) delivers a solution as close to that of the original SCG as desired. Thus, Problem (7.4) may be intuitively interpreted as an ‘‘interpolation’’ between an SCG and the Cournot game. It is well known a Nash-Cournot equilibrium problem can be restated as a VIP (see Scutari et al., 2010). Applying this relationship, we have the following result.

Proposition 7.6. *Under Assumptions 7.1 and 7.2, that a strategy pair $(\tilde{\mathbf{z}}, \tilde{\mathbf{p}}) \in \mathbb{Z} \times \mathbb{P}$ solves Problem (7.4) means it also satisfies the following VI:*

$$\langle \nabla_{\mathbf{z}} l^{(T)}(\tilde{\mathbf{p}}; \tilde{\mathbf{z}}), \mathbf{z} - \tilde{\mathbf{z}} \rangle + \langle c(\tilde{\mathbf{p}}; \tilde{\mathbf{z}}), \mathbf{p} - \tilde{\mathbf{p}} \rangle \geq 0, \quad \forall (\mathbf{z}, \mathbf{p}) \in \mathbb{Z} \times \mathbb{P}. \quad (7.5)$$

If $l^{(T)}(\mathbf{p}; \mathbf{z})$ is convex in \mathbf{z} , then the reverse statement is also true.

In the above VIP, $l^{(T)}$ is a general function represented by DiP. Accordingly, we may solve (7.4) by MD in the same way as we use MD to solve (7.2). This observation entails an algorithm that works as follows (see Algorithm 8 for details). Starting from an initial point, the manager and travelers, each treated as a party in a Cournot game, sequentially update their decisions until convergence. The manager is allowed to anticipate the evolution of travelers' strategy by T steps, which controls how closely the solution approximates that of the original SCG. Proposition 7.6 guarantees that the fixed point of the above algorithm is a solution to (7.4).

Algorithm 8 A single-loop MD (Sil-MD) algoirthm for solving Problem (7.4)

- 1: **Input:** $\mathbf{p}^0 \in \mathbb{P}$, $\mathbf{z}^0 \in \mathbb{Z}$, upper-level learning rate ρ , lower-level learning rate r
 - 2: **for** $i = 0, 1, \dots$ **do**
 - 3: **FP:** Calculate $l^T = l^{(T)}(\mathbf{p}^i; \mathbf{z}^i)$ by calling Algorithm 3.
 - 4: **BP:** Calculate $\mathbf{l}_{\mathbf{z}} = \partial l^T / \partial \mathbf{z}^i$ by calling Algorithm 4 (implemented via AD).
 - 5: **Update both the manager's decision the travelers' strategies:**
 - 6: Set $\mathbf{z}^{i+1} = \arg \min_{\mathbf{z} \in \mathbb{Z}} \rho \cdot \langle \mathbf{l}_{\mathbf{z}}, \mathbf{z} - \mathbf{z}^i \rangle + D_{\psi}(\mathbf{z}, \mathbf{z}^i)$ and $\mathbf{p}^{i+1} = h(\mathbf{p}^i; \mathbf{z}^i)$.
 - 7: If $\delta(\mathbf{p}^i; \mathbf{z}^i) \leq \epsilon$ and \mathbf{z}^i converges, break and set $\tilde{\mathbf{z}} = \mathbf{z}^i$ and $\tilde{\mathbf{p}} = \mathbf{p}^i$.
 - 8: **end for**
-

It is worth emphasizing the essence of Algorithm 8 is co-evolution. By allowing both parties to evolve together toward a fixed point, co-evolution effectively transforms the double-loop algorithm (Algorithm 7) into a single-loop one. Algorithm 8 promises significant computational advantage over Algorithm 7 thanks to its single-loop structure and limited anticipation. As discussed in Section 2.3, the Cournot approximation (7.3) (i.e., $T = 0$, or zero anticipation) is often considered satisfactory in many applications. With limited anticipation ($T > 0$), the solution quality is expected to improve markedly, even with small T .

Remark 7.7 (Termination condition). To run both algorithms, we need a more concrete rule to determine whether an iterate $\mathbf{z}^i \in \mathbb{Z}$ is sufficiently close to the minimizer of the function $l(\mathbf{p}^T; \mathbf{z}^i)$. Recall that both algorithms involve an MD step $\mathbf{z}^{i+1} = \arg \min_{\mathbf{z} \in \mathbb{Z}} \rho \cdot \langle \mathbf{l}_{\mathbf{z}}, \mathbf{z} - \mathbf{z}^i \rangle + D_{\psi}(\mathbf{z}, \mathbf{z}^i)$. The decrement in the objective function value after this MD step is estimated as $\langle -\mathbf{l}_{\mathbf{z}}, \mathbf{z}^{i+1} - \mathbf{z}^i \rangle$. Given a tolerance value $\tau > 0$, we then define the termination condition as

$$\delta^i = -\langle \mathbf{l}_{\mathbf{z}}, \mathbf{z}^{i+1} - \mathbf{z}^i \rangle / \rho < \tau, \quad (7.6)$$

in which the decrement is normalized by ρ . When $\mathbb{Z} = \mathbb{R}^n$, we have $\delta^i = \|\mathbf{l}_{\mathbf{z}}\|_2^2$, the squared ℓ_2 norm of $\mathbf{l}_{\mathbf{z}}$.

8 Multi-Class Extension

The differentiable bilevel programming approach can be easily extended to handle more general settings of SCGs. This advantage is highlighted here with a classical extension of the routing game: the multi-class routing game (Harker, 1988).

In a multi-class routing game, travelers are divided into different classes according to certain characteristics (e.g. value of time). Denote \mathbb{M} as the set of classes and let d_m represent the number of travelers in class $m \in \mathbb{M}$. Similarly, we define $q_m = \Sigma^\top d_m$. The route choice of travelers in class m is represented by a vector $p_m \in \mathbb{P} = \{p \geq 0 : \Sigma p = 1\}$. Accordingly, path flow $f_m = q_m \circ p_m$ and link flow $x_m = \Sigma f_m$. We then denote the link cost experienced by travelers in class m as $u_m = u_m(x; z)$, where $x = (x_m)_{m \in \mathbb{M}}$, and the path cost $c_m = \Lambda^\top u_m$. Denoting $p = (p_m)_{m \in \mathbb{M}} \in \mathbb{P}^{|\mathbb{M}|}$ as the joint route choice of all travelers, $c_m : \mathbb{P}^{|\mathbb{M}|} \rightarrow \mathbb{R}^{|\mathbb{K}|}$ can be defined as $c_m(p; z) = \Lambda u_m(x; z)$, where $x = (x_m)_{m \in \mathbb{M}} = (\Lambda q_m \circ p_m)_{m \in \mathbb{M}}$.

The above setting allows (i) travelers from different classes to experience a different cost on the same link, and (ii) the cost on a link is affected by flows on other links in an asymmetric manner.

Definition 8.1 (WE of a multi-class routing game). A joint route choice $p^* \in \mathbb{P}^{|\mathbb{M}|}$ is a WE of a multi-class routing game if for all $m \in \mathbb{M}$, $w \in \mathbb{W}$ and $k \in \mathbb{K}_w$, we have $c_{m,k}(p^*; z) > \min_{k' \in \mathbb{K}_w} c_{m,k'}(p^*; z) \rightarrow p_{m,k}^* = 0$.

The VIP formulation can be directly extended to handle the multi-class problem (Dafermos, 1980).

Proposition 8.2 (VIP formulation for a multi-class routing game). Letting $c(p; z) = (c_m(p; z))_{m \in \mathbb{M}}$, then a joint route choice $p^* \in \mathbb{P}^{|\mathbb{M}|}$ is a WE if and only if

$$\langle c(p^*; z), p - p^* \rangle = \sum_{m \in \mathbb{M}} \langle c_m(p^*; z), p_m - p_m^* \rangle \geq 0, \quad \forall p \in \mathbb{P}^{|\mathbb{M}|}. \quad (8.1)$$

We next discuss how the proposed framework can be adapted to solve an SCG with a multi-class routing game at its lower level. The key is to reformulate the multi-class routing game as a DiP. Since the ILD operates on the zeroth order (i.e., it needs no more information than travel cost), the extension is straightforward, requiring only to redefine the h function as $h : \mathbb{P}^{|\mathbb{M}|} \times \mathbb{Z} \rightarrow \mathbb{P}^{|\mathbb{M}|}$

$$h_{m,k}(p; z) = \frac{p_{m,k} \cdot \exp(-r \cdot c_{m,k}(p; z))}{\sum_{k' \in \mathbb{K}_w} p_{m,k'} \cdot \exp(-r \cdot c_{m,k'}(p; z))}, \quad \forall k \in \mathbb{K}_w, \quad \forall w \in \mathbb{W} \quad \forall m \in \mathbb{M}. \quad (8.2)$$

Would the dynamics defined by $p^{t+1} = h(p^t; z)$ converge to a WE of the multi-class routing game? Because WE and MCE share the same form of VIP formulation (see Propositions 4.2 and 8.1), we believe the answer is likely yes. That is, Theorem 5.7 may be extended to cover the multi-class case (Recall the proof of Theorem 5.7 does not rely on a specific form of the function $c(p; z)$). However, whether the function $c(p; z) = (c_m(p; z))_{m \in \mathbb{M}}$ is cocoercive might be application specific. We leave a thorough investigation of the convergence issues to a future study.

With the new ILD, all that is left to do is reprogram $h(p; z)$ according to (8.2) in Algorithm 3. The rest will be taken care of by the framework itself, with little additional effort.

Example 8.3 (Mixed autonomy). Assume travelers drive two different types of vehicles: ($|\mathbb{M}| = 2$): connected and autonomous vehicles (CAVs, $m = 1$) and human-driven vehicles (HDV, $m = 2$), and the effective capacity on a given link vary with the share of CAVs using it. Bahrami and Roorda (2020), for example,

suggested the link cost be computed using the following revised Bureau of Public Road (BPR) function:

$$u_{time,a}(x_{1,a}, x_{2,a}) = u_{0,a} \cdot \left(1 + 0.15 \cdot \left(\frac{x_{sum,a}}{(1 + \eta \cdot (x_{1,a}/x_{sum,a})^2) \cdot v_{0,a}} \right)^4 \right), \quad (8.3)$$

where $x_{sum,a} = x_{1,a} + x_{2,a}$ is the sum of CAV and HDV flows on link a , $u_{0,a}$ is the free-flow travel time on link a , $v_{0,a}$ is the capacity when all vehicles on link a are HDVs, and η is a parameter that measures the increase in capacity after all HDVs are replaced by CAVs. Suppose a class-specific toll is levied on link a . That is, CAV and HDV drivers must each pay a different toll to use link a , denoted as $\beta_{1,a}$ and $\beta_{2,a}$, respectively. Thus, the class-specific link cost function reads $u_m(\mathbf{x}_1, \mathbf{x}_2) = u_{time}(\mathbf{x}_1, \mathbf{x}_2) + \gamma \cdot \beta_m$ ($m = 1, 2$), where γ is the time value of money.

9 Numerical Experiments

To test the capabilities of the proposed methodology, we use a few transportation management problems built on a multi-class routing game modeled after Example 8.3 (mixed autonomy). The experiments are structured as follows. Sections 9.1 and 9.2 focus on the computational performance of the forward-propagation (FP) and backward propagation (BP) algorithms, respectively. Essentially, FP solves the multi-class routing game with ILD, and BP calculates the gradient by unrolling ILD with AD. In Section 9.3, we experiment with SCGs on a variety of networks, in which the manager is given one of the following three instruments to mitigate traffic congestion: (i) congestion pricing, cf. Example 4.5; (ii) capacity expansion, cf. Example 4.6, and (iii) directly controlling the paths taken by a subset of CAVs, cf. Example 4.7. Unless otherwise specified, the following settings will be used throughout this section.

1. *Travel demand.* The travel demand by CAVs and HDVs are $\mathbf{d}_1 = \alpha \cdot \mathbf{d}$ and $\mathbf{d}_2 = (1 - \alpha) \cdot \mathbf{d}$, respectively, for a total demand \mathbf{d} and $\alpha \in [0, 1]$. The manager has the authority to control the paths taken by all CAVs, though they may choose to apply the control measure to a subset.
2. *Cost function.* We adopt the revised BPR function (cf. Equation 8.3) and set $\eta = 1$. We note \mathbf{u}_0 can be interpreted as free-flow travel time and \mathbf{v}_0 physical road capacity. The manager may enhance \mathbf{v}_0 at a cost and impose discriminative tolls on CAVs and HDVs on selected links.
3. *Equilibrium gap.* The gap of the multi-class routing game is defined as the maximum over the class-specific (CAV and HDV) relative equilibrium gap, i.e.,

$$\delta(\mathbf{p}_1, \mathbf{p}_2; \mathbf{p}_0) = \max_{m=1,2} \left\{ -\frac{\langle c_m(\mathbf{p}_1, \mathbf{p}_2; \mathbf{p}_0), \mathbf{p}'_m - \mathbf{p}_m \rangle}{\langle c_m(\mathbf{p}_1, \mathbf{p}_2; \mathbf{p}_0), \mathbf{p}_m \rangle} \right\}, \quad \mathbf{p}'_m \in \arg \min_{\mathbf{p}''_m \in \mathbb{P}} \langle c_m(\mathbf{p}_1, \mathbf{p}_2; \mathbf{p}_0), \mathbf{p}''_m \rangle. \quad (9.1)$$

All algorithms are coded using Python 3.9.12 and PyTorch 1.12.0. All numerical results reported in this section were produced either on a MacBook Pro (15-inch, 2017) with 2.9 GHz Quad-Core Intel Core i7 CPU or on a Ubuntu 20.04.4 LTS (GNU/Linux 5.4.0-122-generic x86_64) workstation with NVIDIA RTX A6000 GPU. All codes, both the executable and the source, are included in this paper's electronic companion¹.

¹<https://github.com/jiayangli-nu/Differentiable-Bilevel-Programming>

9.1 Performance of Forward Propagation (FP) Algorithm

We first investigate the performance of FP in the form of ILD. The experiments in this section are designed to answer two questions: (i) would \mathbf{p}^t converge to a WE of the multi-class routing game using ILD?; (ii) how should we choose \mathbf{p}^0 ? For the second question, we hypothesize that $\mathbf{p}^0 = (\mathbf{1}/\Sigma^\top \Sigma \mathbf{1})_{m=1,2}$, i.e., an equal distribution among paths included in \mathbb{K}_w for all $w \in \mathbb{W}$, is a good choice. Experiments in this section will be run on four transportation networks, including Braess (Braess, 1968), Three-Node-Four-Link (3N4L) (Tobin and Friesz, 1988), Sioux-Falls, (Leblanc, 1975) and Chicago-Sketch (Eash et al., 1979). The topology of Braess and 3N4L networks are shown in Figures 2 and 3, respectively. Sioux-Falls has 24 nodes, 76 links, and 528 OD pairs, whereas Chicago-Sketch has 933 nodes, 2950 links, and 93135 OD pairs.

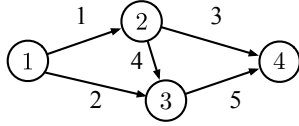


Figure 2: Topology of Braess network.

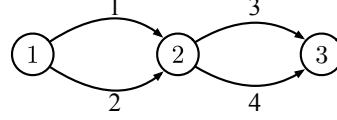


Figure 3: Topology of 3N4L network.

9.1.1 Experiment A: Convergence Rate of ILD

We examine the convergence of \mathbf{p}^t on all networks listed above. We assume the share of CAVs be 20% in all problems, i.e., $\alpha = 0.2$. The initial routing strategy \mathbf{p}^0 is randomly sampled from a uniform distribution and re-scaled to fit the flow conservation condition. The sample size is set as 100 for Braess and 3N4L, and 1000 for the other two. The equal distribution strategy mentioned above is employed as a benchmark. Given a network and a \mathbf{p}^0 , we run the ILD for T iterations (T varies with the network size) with the same learning rate r . The resulting convergence curves (equilibrium gap vs. iteration) are reported in Figure 4.

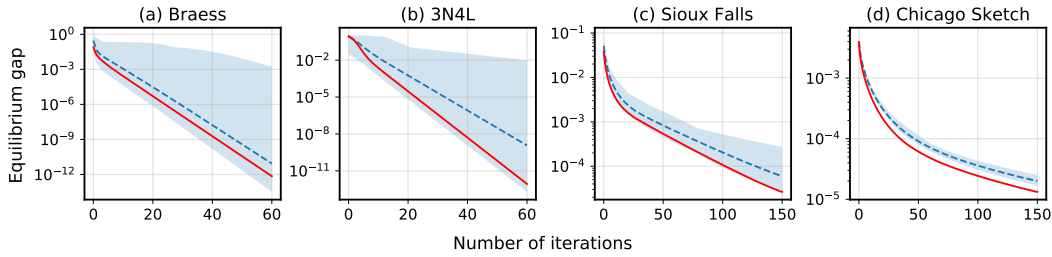


Figure 4: Convergence patterns of the ILD for the four networks. Blue shadow represents the collection of the convergence curves corresponding to all random initial points; the blue dashed line represents the average of the collection; the red solid line represents the curve corresponding to the equal-distribution initial solution.

The results confirm that ILD defined by Equation (8.2) is convergent in the multi-class routing game specified in Example 8.3 for all randomly sampled \mathbf{p}^0 . The convergence rate varies with both the network and the initial solution. Whereas ILD converges almost linearly for Braess and 3N4L, it converges sub-linearly for the two larger networks. Interestingly, the larger the network, the less effect the initial solution seems to have on the convergence performance. The results also indicate the equal-distribution initial solution delivers consistently superior convergence performance. It always outperforms the “average” of all convergence

curves from random initial solutions. In large networks, it is a better point to start the algorithm than any of the one thousand random initial solutions tested. Thus, the evidence strongly supports that starting ILD with an equal-distribution solution is good practice.

9.1.2 Experiment B: Distribution of the Limit Points of ILD

It is well known a multi-class routing game may not have a unique equilibrium. When the followers' best response is not unique in a Stackelberg game, a common strategy in the literature is to adopt either the optimistic or the pessimistic principle, which respectively selects the best or worst solution, as judged by the leader's objective (Loridan and Morgan, 1996). Our approach takes the perspective of the followers instead. It picks a solution corresponding to the followers' route choice behaviors as embedded in ILD. In this experiment, we explore how the final equilibrium reached by such a behavioral principle varies with the initial solution.

We employ Braess and 3N4L networks in this experiment because they each represent a basic building block of more complex networks (3N4L for parallel routes and Braess for parallel routes with a bridge). For simplicity, the total travel time is used as the surrogate to represent an equilibrium solution. We solve the multi-class routing game on both networks for 5000 times, each starting with a different initial solution and running 500 iterations ($T = 500$) to get a sufficiently precise solution. Figure 5 reports the histogram of the total travel times obtained by running ILD. If the multi-class routing game had a unique equilibrium, all 5000 solutions would yield exactly the same total travel time (hence we would observe a Dirac delta distribution). Instead, they spread widely in both cases. Given the equilibrium gap is several orders of magnitude smaller than the range of the distributions, these results are an unmistakable sign of multiple equilibria.

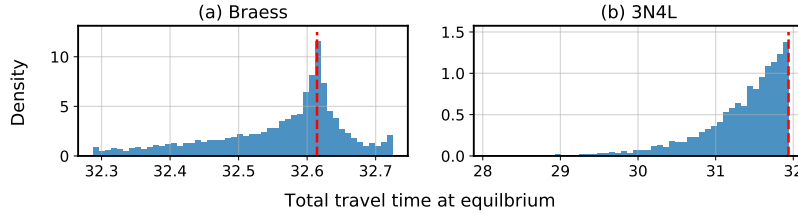


Figure 5: The distribution of the total travel time over the set of equilibria reached by ILD starting from different initial routing strategies. The red, dotted line highlights the total travel time at the equilibrium corresponding to the equal-distribution initial solution.

The two histograms display distinctive patterns. For the Braess network, the histogram seems normal, although it shows a rather prominent left skew. The histogram of the 3N4L network resembles a mirrored exponential distribution. We conjecture the shape of the histogram may be related to network topology and may become closer to normal on more complex networks. The more interesting finding here, however, involves again the equal-distribution initial solution. That is, the equilibrium obtained from this particular initial solution seems to align perfectly with the peak of the histogram in both cases. In other words, *the solution produced by ILD starting from the equal-distribution initial solution may be the most likely equilibrium*. In the literature, the most likely equilibrium of a routing game is characterized by the maximum entropy principle (Boyce and Xie, 2013; Xie et al., 2017). It is easy to verify in these two examples that the equilibrium achieved by ILD from the equal-distribution initial solution indeed maximizes the entropy. The question, of course, is whether this result is mere coincidence or mathematical certainty. While we have

accumulated ample numerical evidence supporting the latter, we believe a rigorous analysis is beyond scope of the present inquiry and should be left to a future study. For now, the findings are sufficiently convincing for us to keep using the equal-distribution initial solution in the remaining experiments.

9.2 Performance of Backward Propagation (BP) Algorithm

We proceed in this section to test the backward propagation algorithm, which is employed to calculate the gradient of the manager’s objective (set as the total travel time hereafter) at the lower level equilibrium. When such equilibrium is unique, the standard method for evaluating the gradient is to recast the equilibrium condition as a fixed-point equation and then perform implicit differentiation (ID), the so-called sensitivity analysis (Tobin, 1986). This method, however, is not directly applicable if uniqueness is absent (Tobin and Friesz, 1988). The BP algorithm in the proposed framework is not subject to this limitation, because the gradient can be calculated from unrolling any equilibrium achieved by FP. In other words, FP defines a computational graph leading to an equilibrium, which BP then unrolls over the same graph. The structure of our BP algorithm is similar to that of Li et al. (2020), though they form FP using a Euclidean projection (EP) algorithm rather than ILD. We perform three experiments. Experiment C verifies the correctness of the proposed BP algorithm using ID as a benchmark. Experiment D compares the computational performance of the proposed algorithm and ID. In Experiment E, the ILD-based backward propagation is compared against the ED-based method of Li et al. (2020). To conduct Experiments D and E, two sets of hypothetical networks are constructed: single O-D networks with non-overlapping parallel routes (see Figure 6) and grid networks (see Figure 7). In both networks, the parameters (e.g., link capacity and demand) are carefully selected to ensure the “overall congestion level” remains roughly unchanged when they scale up.

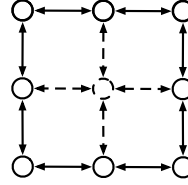
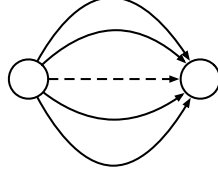


Figure 6: Topology of parallel network. Figure 7: Topology of grid network.

9.2.1 Experiment C: Correctness of Automatic Differentiation

Since the direct application of ID requires at least the total travel time at equilibrium is unique, we shall set $\alpha = 0$ in this experiment (i.e., the share of CAV is zero). This essentially reduces the multi-class routing game to a single-class one. Our objective is to demonstrate the gradients calculated by the proposed BP method and ID are identical. To this end, we first produce an almost exact equilibrium solution (with an equilibrium gap less than 10^{-15}) and then apply ID to obtain the gradient of the total travel time with respect to each link capacity. Then, we run the proposed BP algorithm several times, each over a different computational graph. Recall the computational graph is defined by the number of iterations (T) in FP. The larger T , the closer to the exact equilibrium the solution achieved by FP, and the more precise the gradient calculated by BP. Thus, it is expected, as T increases, the gradient given by the proposed BP algorithm would converge to that by ID.

We conduct the experiment on Braess (Scenario A) and 3N4L (Scenario B) networks because they have representative topology. Notably, the equilibrium path flow is unique for Braess but not for 3N4L, even

though the total travel time is unique in both cases. As a result, the standard path-based ID method can only be applied for Braess. For the 3N4L network, we apply Tobin (1986)’s ID method on a link-based VI formulation of the single-class routing game, as suggested by Patriksson and Rockafellar (2002).

Table 1: Gradients of total travel time with respect to link capacity, obtained by the proposed BP algorithm (with different T) and ID.

(i) Scenario A: Braess network.						(ii) Scenario B: 3N4L network.				
Method	link 1	link 2	link 3	link 4	link 5	Method	link 1	link 2	link 3	link 4
AD ($T = 0$)	-19.2	-0.06	-0.06	-9.60	-19.2	AD ($T = 0$)	-14.20	-71.01	-1410	-8.582
AD ($T = 10$)	-1.92	-0.50	-0.50	0.47	-1.92	AD ($T = 4$)	-35.01	-23.35	-109.6	-45.86
AD ($T = 20$)	-2.30	-0.47	-0.47	0.12	-2.30	AD ($T = 8$)	-35.17	-23.44	-108.7	-46.32
ID	-2.31	-0.47	-0.47	0.12	-2.31	ID	-35.17	-23.44	-108.7	-46.32

Table 1 compares the gradients calculated by the proposed BP algorithm over a computational graph associated with different values of T . The results confirm the proposed BP algorithm obtains gradients almost identical to that obtained by ID when T is sufficiently large. For 3N4L, the differences between the gradients achieved by the proposed algorithm and ID become negligible once T reaches 8. For Braess, the value of T required to achieve this level of precision is 20. Thus, the larger T in the FP of the proposed algorithm, the more precise the equilibrium solution obtained, and the more accurate the derivatives obtained from the BP.

9.2.2 Experiment D: Automatic Differentiation v.s. Implicit Differentiation

To test the scalability of the proposed algorithm relative to ID, a set of parallel networks — with $|\mathbb{A}|$ varying from 10^1 to 10^6 — are employed (Figure 6). By ensuring path flow uniqueness, the special topology allows us to perform ID in the most straightforward way, which makes the comparison more favorable to ID than that over networks with a more general topology. To directly apply ID, we still need to focus on single-class games (i.e., $\alpha = 0$). For all tested networks, we first run FP until the relative equilibrium gap is below 10^{-3} . The equilibrium solution is then fed to both the proposed BP algorithm and ID to calculate the gradient of the total travel time with respect to link capacity. Table 2 reports the results, including the total number of iterations required to reach the convergence criterion, as well as the GPU time consumed by FP, BP, and ID. The results of ID are not reported on networks with $|\mathbb{A}| > 10^4$ because the test machine would either run out of memory (if GPU is used) or take too long (if CPU is used) on these networks.

Table 2: Computational performance of the proposed BP algorithm and ID for gradient evaluation on single-OD networks with parallel routes (T_{iter} and FP time represent, respectively, the number of iterations and GPU time required by FP to reach an equilibrium gap of 10^{-3}).

$ \mathbb{A} = \mathbb{K} $	10^1	10^2	10^3	10^4	10^5	10^6
T_{iter}	15	40	49	80	67	65
FP time (s)	0.0113	0.0326	0.0415	0.0800	0.110	0.338
BP time (s)	0.0203	0.0382	0.0484	0.0718	0.0752	0.297
ID time (s)	0.0116	0.0975	0.933	15.2	-	-

As the network size increases, the number of iterations and GPU time required by FP to reach the convergence criterion does not increase much. Similarly for BP, the GPU time scales sub-linearly with the network size.

When $|\mathbb{A}|$ is changed from 10 to 10^6 (an increase of 100,000 folds), BP time increase by a factor of about 15. This is in sharp contrast with ID time, which scales super-linearly with the network size. For the network with 10,000 links, the proposed BP algorithm is already 200 times faster than ID, and the difference is expected to grow fast on larger networks. It is tempting to simply attribute the superior performance of the proposed algorithm to its avoiding the inversion of a matrix of size $|\mathbb{A}|^2$ (as required by ID). However, a closer look reveals the key is the relatively small number of iterations T_{iter} , which equals the depth of the computational graph. In the smallest network ($|\mathbb{A}| = 10$), where $T_{\text{iter}} < |\mathbb{A}|$, ID is in fact faster than the proposed algorithm. Only after $|\mathbb{A}|$ exceeds T_{iter} does the performance of the two algorithms begin to diverge. Indeed, whereas the calculation of ID is dominated by matrix inversion, which scales with $|\mathbb{A}|^2$, that of the proposed algorithm scales with $|\mathbb{A}|T_{\text{iter}}$. Thus, as long as T_{iter} is smaller than the size of the matrix that ID must invert — a condition satisfied by most practical routing games — the proposed method is expected to enjoy greater scalability. It is worth noting that T_{iter} is more sensitive to the level of congestion (demand-to-capacity ratio) than to network size. Thus, the advantage of the proposed algorithm relative to ID might be eroded in more congested problems.

9.2.3 Experiment E: Unrolling ILD v.s. Unrolling EP

We move to compare the proposed BP algorithm with the BP method in Li et al. (2020). Recall the difference between the two lies in FP: an EP-based algorithm in Li et al. (2020) vs. ILD in this study. For this purpose, a set of grid networks (Figure 7), which better mimic a real road network, are used. We also return to multi-class routing by setting $\gamma = 0.2$. The number of nodes in the network is gradually increased from 10×10 to 50×50 . In all five networks, the convergence criterion is set to 10^{-4} for FP, which determines the depth of the computational graph for both methods. Li et al. (2020)’s method is implemented with a special python package called `cvxpylayers` (Agrawal et al., 2019), which is in turn built on the python version of the classic solver CVX (Diamond and Boyd, 2016). As CVX does not support GPU, it is only run on CPU. Table 3 compares the total number of iterations required by FP to reach the desired convergence criterion, as well as the running time of FP and BP by both methods. Due to unreasonably high computation time, the method proposed by Li et al. (2020) is not tested on networks with $|\mathbb{N}| \geq 30 \times 30$.

Table 3: Computational performance of FP and BP by ILD (the proposed algorithm) and EP (Li et al., 2020). $|\mathbb{N}|$: number of nodes; $|\mathbb{K}^*|$: number of paths used at equilibrium; N_{link} : average number of links per path; T_{iter} : total number of iterations of FP before convergence.

Method	$ \mathbb{N} $	10×10	20×20	30×30	40×40	50×50
	$ \mathbb{K}^* $	259	4167	25646	88507	340800
	N_{link}	7.19	15.22	23.57	31.15	39.19
ILD	T_{iter}	31	39	62	73	89
	FP CPU/GPU time (s)	0.0136/0.200	0.168/0.273	2.31/0.61	13.4/1.57	55.1/7.01
	BP CPU/GPU time (s)	0.0122/0.193	0.179/0.266	2.47/0.63	11.0/1.68	65.6/8.32
	T_{iter}	40	22	-	-	-
EP	FP CPU time (s)	0.984	18.2	-	-	-
	BP CPU time (s)	1.47	198	-	-	-

The results suggest the two algorithms, ILD and EP, are comparable in terms of convergence speed as measured by T_{iter} . However, the execution speed is much faster with ILD than with EP, for both FP and BP.

Take the 20 by 20 network. ILD is nearly two orders of magnitude faster than EP for FP and nearly three orders of magnitude faster than EP for BP. This dramatic speedup can be attributed to the simple analytical form enjoyed by ILD, which is much easier to evaluate than repeatedly solving quadratic programs by calling CVX. Another observation from the table is the difference between using GPU and CPU in ILD (EP must use CPU, as explained above). For smaller networks ($|\mathbb{N}|$ is 20 by 20 or less), CPU is slightly faster. However, on large networks, the advantage of GPU computation is unequivocal: it cuts the calculation time by nearly 90% on the 50 by 50 network.

Table 3 also indicates that ILD-based FP and BP may scale much better in practice than predicted by the analysis given in Section 6, especially when GPU is fully utilized. According to that analysis, the running time would increase linearly with $T_{\text{iter}} \cdot |\mathbb{K}^*| \cdot N_{\text{link}}$ for both ILD-based FP and BP. If so, dividing the sum of FP and BP running time by $T_{\text{iter}} \cdot |\mathbb{K}^*| \cdot N_{\text{link}}$ would roughly yield 1:1:1:1:1 for the five networks. Instead, we get 68: 2.2: 0.33: 0.16: 0.13 (based on the GPU time reported in Table 3), indicating a sublinear scale with $T_{\text{iter}} \cdot |\mathbb{K}^*| \cdot N_{\text{link}}$ as $|\mathbb{N}|$. This better-than-expected performance is achieved in part because ILD can be coded as an array program (see Algorithm 5 for an example), which enables it to better take advantage of parallel computing capabilities available on modern computers (including the use of GPU). We should note acceleration provided by parallel computing has its limit. First, it cannot save memory consumption, which is expected to grow linearly with $T_{\text{iter}} \cdot |\mathbb{K}^*| \cdot N_{\text{link}}$. Second, the computational cost still grows linearly with T_{iter} , as the calculations taking place in different iterations must be processed sequentially, not in parallel.

To briefly sum up, the above three experiments verified that AD can accurately and efficiently calculate the gradient of the manager’s cost at equilibrium. They also confirmed the superiority of Algorithm Dol-MD over classic ID (sensitivity analysis) based methods (Friesz et al., 1990) and Li et al. (2020)’s AD-based methods in terms of computational efficiency. In the next section, we compare Dol-MD and Sil-MD over a set of classic SCG games to demonstrate what co-evolution and limited anticipation — the key features of Sil-MD — can do to further speed up the computation.

9.3 Performance of Stackelberg Congestion Game (SCG) Algorithms

We investigate the performance of Dol-MD (Algorithm 7) and Sil-MD (Algorithm 8) in solving three classical SCGs: the continuous network design problem on the Braess network (Experiment F), the second-best congestion pricing problem on the Sioux-Falls network (Experiment G), and the CAV route control problem on the Chicago-Sketch network (Experiment H). To the extent possible, we benchmark the solutions obtained by our algorithms with those from the literature. We focus on the single class setting in Experiments F and G (i.e., $\alpha = 0$) to be consistent with the literature, before switching back to multi-class in Experiment H. Unless otherwise specified, the same hyperparameters, including the initial solution z^0 and p^0 , the learning rates (ρ in the upper level and r in the lower level) as well as the tolerance values (τ for the upper level and ϵ for the lower level), are employed for Dol-MD and any version (identified by the value of T) of Sil-MD in each experiment, respectively. Throughout this section, we shall define the cooperative equilibrium (CE) of a routing game as the solution that minimizes the total travel time, often known as Wardrop’s second principle.

9.3.1 Experiment F: Continuous Network Design on the Braess Network

The Braess network has three paths connecting node 1 (the origin) and node 4 (the destination), cf. Figure 2. Let us say path 1 uses links 1 and 3, path 2 uses links 1, 4, and 5, and path 3 uses links 2 and 5. Recall in

Example 4.6 the manager can add a vector of extra link capacities, denoted as $z \in \mathbb{R}_+^5$, at a monetary cost $m(z) = \langle w, z^2 \rangle$. We assume $w \in \mathbb{R}_+^5$ be proportional to link length and the manager aim to minimize a weighted sum of the total travel time and the monetary cost.

It is well known that expanding the capacity on link 4 (the bridge link) in the Braess network is counter-productive, as it will increase the total travel time at WE (Braess, 1968). Therefore, we expect the optimal capacity expansion scheme would forbid adding new capacities to that link. To stress this point, we test two scenarios: (A) capacity expansion on link 4 is explicitly forbidden, i.e., $\mathbb{Z} = \{z \in \mathbb{R}_+^5 : z_4 = 0\}$; and (B) capacity expansion is permitted on all links, i.e., $\mathbb{Z} = \mathbb{R}_+^5$. For each scenario, the problem is solved by four algorithms: Dol-MD, Sil-MD (with $T = 0, 1, 3, 6, 10$), the iterative optimization-assignment (IOA) algorithm (Marcotte and Marquis, 1992), and the socially optimal (SO) scheme that assumes all travelers work cooperatively with the manager (Dantzig et al., 1979). Since IOA solves the Cournot game model (7.3) as an approximation, it, in theory, equals Sil-MD when $T = 0$ (i.e., the manager forgoes anticipation altogether), and yields an upper bound to the original SCG. On the other hand, the SO solution provides a lower bound. For simplicity, we shall abbreviate Dol-MD as D and abbreviate Sil-MD with $T = 0, 1, 3, 6, 10$ as S-0, S-1, S-3, S-6, and S-10. Table 4 reports the solutions (upper-level: capacity enhancement; lower-level: routing strategy) and the corresponding objective function values.

Table 4: Capacity enhancement and routing solutions obtained by Dol-MD (Algorithm 7), Sil-MD (Algorithm 8; $T = 0, 1, 3, 6, 10$), IOA and SO on the Braess network.

(i) Scenario A: capacity enhancement is forbidden on link 4.									
Method	Objective	Upper-level: Capacity enhancement					Lower-level: Routing strategy		
		$a = 1$	$a = 2$	$a = 3$	$a = 4$	$a = 5$	$k = 1$	$k = 2$	$k = 3$
S-0	29.0194	1.081	0.010	0.010	0	1.081	0.3365	0.3270	0.3365
S-1	28.9799	0.818	0.020	0.020	0	0.818	0.3426	0.3148	0.3426
S-3	28.9254	0.896	0.018	0.018	0	0.896	0.3405	0.3191	0.3405
S-6	28.9200	0.938	0.016	0.016	0	0.938	0.3395	0.3211	0.3395
S-10	28.9198	0.932	0.016	0.016	0	0.932	0.3396	0.3208	0.3396
D	28.9198	0.929	0.016	0.016	0	0.929	0.3333	0.3333	0.3333
IOA	29.0176	1.079	0.010	0.010	0	1.079	0.3365	0.3269	0.3365
SO	26.7298	0.812	0.032	0.032	0	0.812	0.4281	0.1438	0.4281

(ii) Scenario B: capacity enhancement is allowed on all links.									
Method	Objective	Upper-level: Capacity enhancement					Lower-level: Routing strategy		
		$a = 1$	$a = 2$	$a = 3$	$a = 4$	$a = 5$	$k = 1$	$k = 2$	$k = 3$
S-0	38.7860	2.075	0.000	0.000	2.828	2.075	0.0000	1.0000	0.0000
S-1	28.9799	0.818	0.020	0.020	0	0.818	0.3426	0.3148	0.3426
S-3	28.9254	0.896	0.018	0.018	0	0.896	0.3405	0.3191	0.3405
S-6	28.9200	0.938	0.016	0.016	0	0.938	0.3395	0.3211	0.3395
S-10	28.9198	0.932	0.016	0.016	0	0.932	0.3396	0.3208	0.3396
D	28.9198	0.929	0.016	0.016	0	0.929	0.3333	0.3333	0.3333
IOA	38.7860	2.075	0.000	0.000	2.828	2.075	0.0000	1.0000	0.0000
SO	26.7217	0.825	0.030	0.030	0.113	0.825	0.4237	0.1527	0.4237

We first note that the SO objective value is slightly higher in Scenario A than in Scenario B. This is expected, because Scenario B may be viewed as a relaxation of Scenario A ($\{z \in \mathbb{R}_+^5 : z_4 = 0\} \subset \mathbb{R}_+^5$). Notably,

link 4 should be expanded under SO, contrary to the expectation of those who are familiar with the Braess paradox. This, however, is an artifact of the SO formulation in which the equilibrium constraint is ignored. As expected, the SO objective value is always the lowest across the board in each scenario.

For the following reasons, the solutions obtained by D will be treated as the optimal solution to the original problem. First, we set the equilibrium tolerance $\epsilon = 10^{-8}$ to get a highly precise approximation of the lower level solution in each iteration. Second, the upper-level tolerance value τ is set to 10^{-4} to secure high-quality local minimums. Last but not least, we repeated the algorithm with more than 100 different initial points, and the convergence to these same solutions was consistent.

It is easy to verify that S-0 and IOA do produce identical results in both scenarios, as suggested by the analysis. What is surprising, however, is how much the solutions produced by them were changed by the capacity enhancement restriction on link 4. With the restriction, the solution given by S-0/ IOA is fairly close to that given by D (the presumed optimal solution). When that restriction is lifted, however, S-0 and IOA wandered off course wildly. Rather than staying away from link 4, they advise investing heavily on that link (with an extra capacity of 2.8). As a result, all travelers were directed to path 3 (which contains links 1, 4, and 5), the very path that should be avoided to resolve the Braess paradox, which in turn produces an objective function value nearly 35% worse than that in Scenario A (with the restriction). Interestingly, as long as we set $T > 0$ in Sil-MD (i.e., with some anticipation), the severe distortion is averted. From Table 4, we see the solutions delivered by S-1, S-3, S-6, and S-10 are identical under both scenarios. Moreover, the solutions evidently converge to the optimal solution when T increases. When T reaches 10, the discrepancy between S-10 and D becomes almost negligible. This result highlights the peril of approximating an SCG by its Cournot counterpart and the importance of (at least partially) anticipating travelers' response.

Table 5: Computational performance of the tested algorithms in Scenario A of continuous network design on the Braess network.

	IOA	S-0	S-1	S-3	S-6	S-10	D
Objective value	29.0176	29.0194	28.9799	28.9254	28.9200	28.9198	28.9198
Total CPU time (s)	0.220	0.206	0.310	0.514	0.812	1.122	1.610
Iteration number	-	432	495	476	518	507	536
Time per iteration (ms)	-	0.48	0.63	1.08	1.57	2.21	3.00

Table 5 reports statistics related to the computation performance, including the total CPU time, the total iteration number, and the CPU time per iteration. We focus on Scenario A as the results for Scenario B are similar. We first note that the total CPU times consumed by IOA and S-0 are comparable. Again, this is expected given their similarities. The results reveal that Dol-MD and Sil-MD took a similar number of iterations to reach the same level of precision. However, the running time per iteration required by Sil-MD is significantly lower than Dol-MD, especially when T is small. In general, Sil-MD is more efficient than Dol-MD. Even S-10, the most time-consuming version of Sil-MD, is still 30% faster than Dol-MD while sacrificing virtually nothing in terms of solution quality. Also worth noting is the fact that, while the CPU time grows with T for Sil-MD, the rate of increase appears to be sublinear. When T is increased from 1 to 10, for example, the CPU time only grew about 5.2 times. Overall, Sil-MD balances the tradeoff between solution quality and computational efficiency better than Mil-MD.

Marcotte (1986) observed that the Cournot game model often approximates the continuous network design model reasonably well, and the efforts to improve the accuracy of this approximation scheme usually introduce such complexity that more than offsets the benefits they provide. The small experiment above seems to have

uncovered a counterexample, in which the error of this approximation becomes unacceptably large. To be sure, the problem is unlikely to be this acute in a general real-world network, and the approximation of an SCG by a Cournot game may still constitute a sound scheme in most networks one may encounter in real applications — our experiment did nothing to disprove such a claim. Nevertheless, Sil-MD still offers an appealing alternative to IOA, simply because it seems capable of avoiding the trap IOA is demonstrably prone to, at the expense of small computational overhead.

9.3.2 Experiment G: Second-Best Congestion Pricing on the Sioux-Falls Network

The second-best congestion pricing problem tested here is based on [Lawphongpanich and Hearn \(2004\)](#), in which the “tollable” links — the links on which levying toll is allowed — are selected based on a simple heuristic scheme. Specifically, they first obtain WE and CE assignment solutions, and then designate a link as tollable if the relative discrepancy between its flow at the WE and that at the CE is greater than a predetermined threshold ξ . In this experiment we focus on two different values of ξ used in [Lawphongpanich and Hearn \(2004\)](#) to create different sets of tollable links: $\xi = 0.05$ (Scenario A, 18 tollable links) and $\xi = 0.15$ (Scenario B, 4 tollable links). The system travel time at the CE and the WE solutions are 71.9426 and 74.8023, which respectively form a lower bound and an upper bound for the problem. [Lawphongpanich and Hearn \(2004\)](#) reported for Scenario A a minimum system travel time of 72.6238, with a corresponding lower bound of 72.1036, achieved after 1743.38s of CPU time; and for Scenario B, the minimum system travel time, the lower bound and the CPU time are, respectively, 73.8787, 73.0681 and 184.78s.

We test Dol-MD and Sil-MD with $T = 1, 3, 6, 10, 15$ in this experiment, abbreviated as D, S-1, S-3, S-6, S-10, and S-15. Note that the IOA method is not applicable in this problem because the manager’s objective function (the total travel time) depends only on the travelers’ routing strategy, not on the decision variables (the link toll level). In other words, once travelers’ routing strategy is fixed from solving the lower level problem, the manager’s cost is fixed and can no longer be improved. Due to the same reason, neither can Sil-MD with $T = 0$ be applied (hence T starts from 1 here).

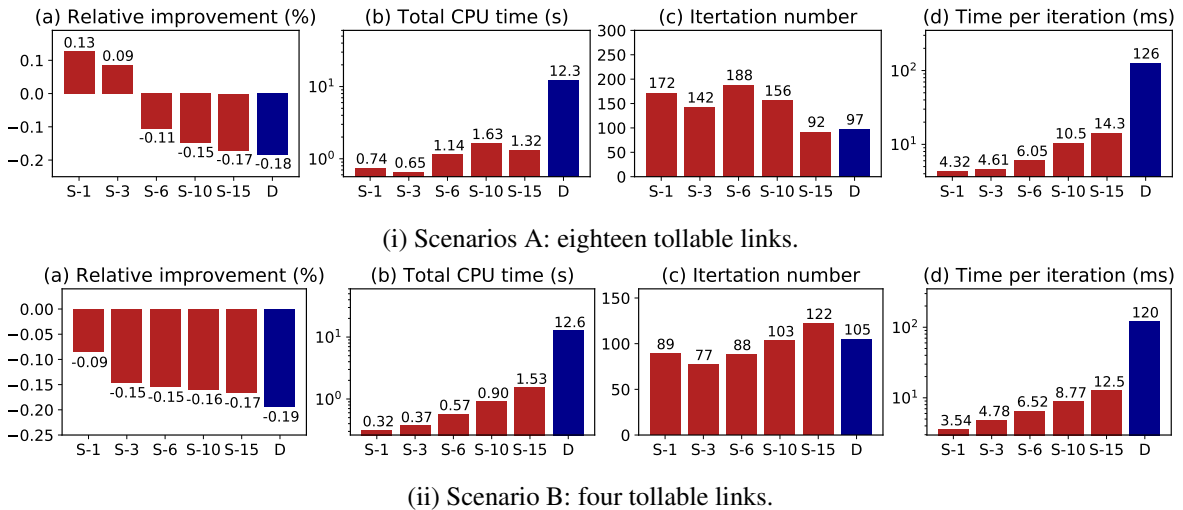


Figure 8: Performance of Dol-MD and Sil-MD (with $T = 1, 3, 6, 10, 15$) for solving the second-best congestion pricing problem on the Sioux-Falls network in two different scenarios.

Figure 8 (i)-(a) and (ii)-(a) report the relative improvement achieved by Dol-MD and Sol-MD, using the optimal solution obtained from [Lawphongpanich and Hearn \(2004\)](#) as the reference point, in Scenarios A and B, respectively. In Scenario A, Algorithm D found a solution that is 0.18% better than the benchmark. Given the relative gap reported for the benchmark solution is about 0.9%, our solution represents a substantial improvement. The relative quality of the solution obtained by Sil-MD depends on T : it outperforms the benchmark by 0.11% when $T = 6$ and falls behind by 0.09% for $T = 3$. S-15 delivers a solution with a quality comparable to that of D. In Scenario B, however, even S-1 beats the benchmark by 0.09%, although the maximum improvement (about 0.19%) is similar.

From Figures 8 (i)-(b) and (ii)-(b) we can see D achieves a slightly better solution than the benchmark with about 12 - 14 seconds of CPU time, whereas the CPU time needed by all versions of Sil-MD is less than two seconds. Interestingly, increasing T does not always result in longer computation time for Sil-MD, evidently because a large T may reduce the total number of outer iterations needed to converge (see Figures 8 (i)-(c), (i)-(d), (ii)-(c), (ii)-(d)). Another observation is that each outer loop takes an order of magnitude more CPU time to finish for D than for any of the Sil-MD implementations. This is not surprising given that D is committed to full anticipation, i.e., solving the lower level to a highly precise WE in each iteration. Since the quality of the solutions given by S-15 and D are very close in both scenarios, the advantage of Sil-MD, in this case, seems indisputable.

Our best-performed algorithm, S-15, solves Scenarios A and B in 1.36s and 0.36s, respectively, representing a speedup of nearly 1000 times over the computational performance reported in [Lawphongpanich and Hearn \(2004\)](#) for their cutting-plane algorithm. Of course, we are far from comparing apple to apple here. First and foremost, the cutting-plane algorithm is specifically tailored to the second-best pricing problem, and capable of assessing solution quality (by solving a relaxed master problem). In contrast, ours is a general-purpose local algorithm based on gradient descent. The fact that our algorithms were able to find better solutions than the cutting-plane algorithm in these experiments does not prove they can always do so in other SCGs. Second, these experiments were performed on computers separated from each other for almost twenty years. Specifically, [Lawphongpanich and Hearn \(2004\)](#) employed a 300 MHz IBP SP2 computer whereas our machine has a 2.9 GHz Quad-Core Intel Core i7 CPU. Judged by the CPU speed alone, we estimate the computation time required to obtain the benchmark solutions would be reduced by an order of magnitude had the cutting-plane algorithm been tested on our computer. Although this would still give our algorithms a significant lead in terms of efficiency, the reader should be aware of the crudeness of such estimation, due to the complexity of the factors affecting computation time that our analysis does not account for.

9.3.3 Experiment H: Stackelberg Routing Problem on the Chicago-Sketch Network

In this experiment we assume 20% of all vehicles are CAVs ($\alpha = 0.2$) whose routes can be controlled by the manager to minimize the system travel time. [Yang et al. \(2007\)](#) studied a variant of this problem, though in their model no asymmetric interactions exist between different types of vehicles at the link level. The Stackelberg routing problem is computationally challenging because both the upper- and lower-level decision variables are route choices that scale with the number of paths in the network and are constrained by the probability simplex. In contrast, the upper-level decision variables in the previous two examples scale with the number of links and are subject only to non-negative constraints. In the literature, this problem is often solved using the Cournot game approximation (e.g., [Van Vuren and Watling, 1991](#); [Zhang and Nie, 2018](#)). However, because the manager cannot fully take advantage of the partial control they have over route choices, such approximation often produces sub-optimal solutions ([Yang et al., 2007](#)).

Since the Chicago-Sketch network is known to have a low level of congestion, we uniformly scale its original OD matrix up by a factor of three to produce meaningful differences between WE and CE solutions. With the scaled demand, the total system travel time at WE and CE are 4211544 and 4087372, respectively. To create a path set that covers the optimal solution to the Stackelberg routing problem, we adopt a simple heuristic that merges the optimal paths corresponding to WE and CE solutions obtained using a path-based algorithm (Xie et al., 2018). This strategy produces 435806 paths or 4.68 per OD pair.

To improve computational efficiency, we may focus only on a subset of OD pairs that have the greatest potential to reduce traffic congestion had their CAVs been subject to control. To rank OD pairs based on this potential, we assume all CAVs be controllable. This means p_1 and p_2 (the routing strategy of CAVs and HDVs) are respectively the upper- and lower-level decision variables. We initialize p_1 as the route choice strategy of CAVs at WE when all vehicles freely make route choices. Using that initial solution, a full iteration of Dol-MD is performed to obtain the gradient of the upper-level objective with respect to p_1 , which measures the sensitivity of the total system travel time to each entry in p_1 . To obtain the potential for travel time reduction by a given OD, we perform a mirror descent on the choice strategy of the paths associated with that OD pair alone, based on the gradient with respect to p_1 . Then the potential of the OD pair can be estimated from the change in the total travel time corresponding to the update. The OD pairs can then be ranked according to their potential. Figure 9 visualizes the top twenty high potential OD pairs.

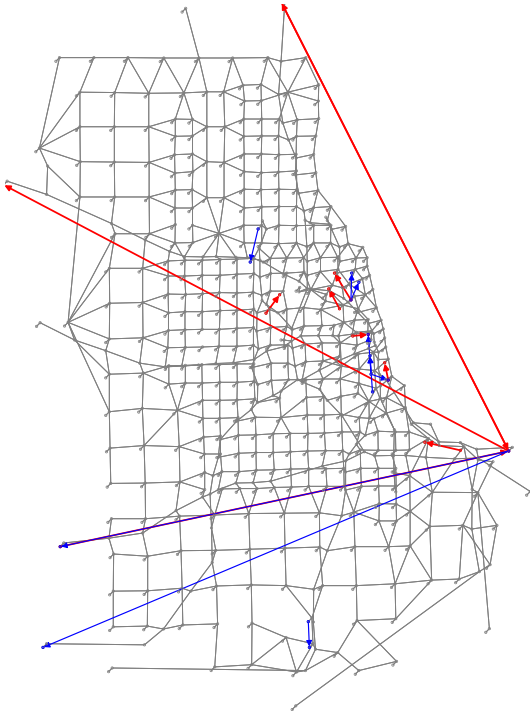


Figure 9: Top twenty OD pairs with high potentials for travel time reduction (red and blue arrows respectively represent the top 1–10 and the top 11–20).

Most of these OD pairs either correspond to long travel distance travel (possibly representing “external” traffic moving through Chicago) or are associated with the more congested downtown area. Given the definition of OD potential, a simple greedy heuristic is to pick the top- K OD pairs based on their potentials. This is sufficient for our purpose, since the focus here is on computational efficiency, not locating a high-quality solution to the Stackelberg routing problem. In what follows, we consider two scenarios. Scenario A assumes the manager only controls the CAVs for the top 4000 OD pairs – or 5.85% of all vehicles – that collectively use 18590 paths. In Scenario B, the top 8000 OD pairs, or 7.38% of all vehicles that use 39642 paths, are controlled. In both cases, the size of the lower-level decision variable (the routing strategy of HDVs and the free CAVs) is 871612.

Solving an SCG of this size is a stretch for Dol-MD, largely due to the large amount of memory needed to store the computational graph (note that a single path-demand incidence matrix Λ contains more than 7 million nonzero elements). This problem is mitigated in Sil-MD because we can limit the depth of the computational graph by setting T to a small

value. In this experiment, we set $T = 0, 1, 3, 6, 10$, referred to as S-0, S-1, S-3, S-6, and S-10, respectively. Due to the scale of the problem, GPU is used in the computation.

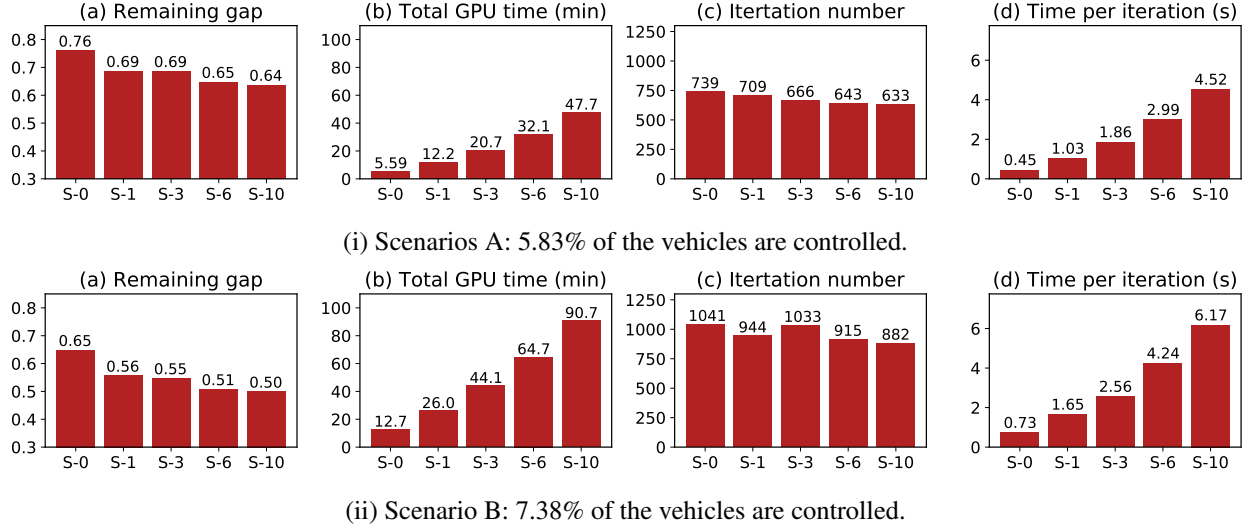


Figure 10: Performance of Sil-MD (with $T = 0, 1, 3, 6, 10$) for solving the Stackelberg routing problem on the Chicago-Sketch network under two different scenarios.

Figures 10-(i)-(a) and (ii)-(a) compare the “remaining gap” achieved by a given implementation of the Sil-MD algorithm in the two scenarios. The remaining gap is defined as the difference between the total travel time at a given solution divided by that between WE and SO. Thus, the smaller the remaining gap, the closer a solution to SO, the better. The best-performed version, S-10, achieved a remaining gap of 0.64 in Scenario A and 0.5 in Scenario B. Thus, by controlling less than 8% of all vehicles, the manager can cut the extra delay caused by selfish routing behavior in half. This result is not surprising. It is well known that much efficiency can be gained by manipulating the route choice of a tiny minority of vehicles (see e.g. [Zhang and Nie, 2018](#)). Also, even the crudest algorithm, S-0, realized more than two-thirds of the improvement gained by S-10. However, the most notable observation here is that, in both scenarios, the reduction in the remaining gap is much larger from S-0 to S-1 than from S-1 to S-10. This highlights the high payoff of having just the minimum level of anticipation (i.e. $T = 1$). As T increases from 1, the benefits of additional anticipation diminish quickly.

Figures 10-(i)-(b-d) and (ii)-(b-d) show the total GPU time required to solve the problem increases with T at a sublinear rate, though the GPU time per iteration is linearly proportional to T . In Scenario A, for example, the total GPU time rose from 12.2 minutes at $T = 1$ to 47.7 minutes at $T = 10$. Also, the GPU time needed for solving Scenario B roughly doubles that for Scenario A, because the size of the upper-level decision variables in Scenario B is about twice as many. If the manager is willing to settle for S-1, it takes less than 30 minutes to find a control strategy that reduces traffic congestion by more than 40%. Considering the scale of the network and the inherent complexity of SCG, such performance is quite encouraging.

10 Conclusions

The recent advances in ML have revealed the great potential of differentiable programming in many applications ([Hu et al., 2019](#); [Jin et al., 2020](#); [Agrawal et al., 2019](#); [Liu et al., 2021](#)). This study attempts to marry

these latest developments with traditional methodologies — notably bilevel optimization and game theory — to forge an integrative approach to attacking large-scale Stackelberg congestion games (SCGs) that often arise in transportation, energy, and other domains. Below, we first summarize the contributions and findings, before commenting on future research.

We revisited a classic evolutionary game theoretic model characterized by the imitative logit dynamics (ILD) and gave sufficient conditions that guarantee the convergence of ILD to the lower-level equilibrium in an SCG. To the best of our knowledge, these convergence conditions are weaker than previously known results.

We demonstrated how automatic differentiation (AD) could be deployed to perform sensitivity analysis in bilevel formulations of SCGs. Unlike the conventional approach, which requires an implicit differentiation of equilibrium conditions, ours explicitly unrolls the ILD trajectory through which the equilibrium is reached. This novel scheme gives rise to a double-loop mirror descent (Dil-MD) algorithm that bears a semblance to conventional methods based on sensitivity analysis. It decomposes the solution of an SCG into two tasks: predicting the performance of the leader’s decision and refining that decision using the gradient information. Among these two tasks, the first is usually considered the “easy” one, thanks to the availability of highly efficient traffic assignment algorithms. Our analysis further reveals, both analytically and numerically, that the complexity of the second task is almost identical to that of the first with the proposed computational architecture that centers on unrolling the ILD by AD.

We discovered that anticipating the followers’ best response — the response at WE — may be an unnecessary, self-imposed computational obstacle. Instead, the leader may only look ahead along the followers’ evolution path for a few steps, while updating their decisions in sync with the followers’ decisions through a co-evolution process. The resulting single-loop mirror descent (Sil-MD) algorithm is much more efficient than Dil-MD, in terms of both memory consumption and computation time. Through numerical experiments that cover a wide range of benchmark problems, we found that Sil-MD consistently strikes a good balance between solution quality and efficiency, outperforming not only Dil-MD but also other methods from the literature. Importantly, our results highlighted both the wastefulness of “full anticipation” and the peril of “zero anticipation”. If a “quick-and-dirty” heuristic is needed for solving a really large SCG, we recommend applying Sil-MD with $T = 1$ — that is, the leader only anticipates the followers’ evolution by one step — as a replacement for the popular iterative-assignment algorithm (or Cournot game approximation).

This study can be extended in many directions. The current framework, especially the concept of limited anticipation and co-evolution, hints at the possibility of further weakening or even abandoning the “equilibrium-centric” point of view, at least in many transportation applications, where the lower-level problem is defined not so much by equilibrium conventionally construed as by continuous evolution of travel choices. Our framework would fit a behavior-centric approach perfectly since the ILD can be easily replaced with another evolutionary dynamical process that embeds any travel behaviors deemed suitable in a given application context. In this regard, the flexibility offered by our framework seems unlimited. The challenge still resides with the issue of convergence. Would a given dynamical process converge to a stationary point? How should we interpret such stationary points? Could we use them as a reference point to evaluate alternative designs and policies, the same way transportation planners had been using WE for such purposes? These are the questions that future studies need to answer.

The proposed algorithms, both Dil-MD and Sil-MD, rely on pre-defined path sets that supposedly cover all WE paths used at the optimal solution of the SCG. This is not necessarily a hard constraint on their practical applications (as generating such paths can be done quite efficiently even on very large networks) but nonetheless an undesirable feature. A future study can endogenize path generation by adding a column-

generation procedure. Finally, we have uncovered strong evidence that the ILD can reach a maximum-entropy (ME) WE solution if starting from an equal-distribution initial point. If proven true, this finding would provide a highly efficient and flexible alternative to existing approaches to finding the ME-WE path solution. Given the importance of path flow uniqueness in some transportation planning applications (e.g., select link analysis), an in-depth investigation of this issue would be of both theoretical and practical interest.

A Proofs in Section 5

A.1 Proof of Proposition 5.4

The following lemma (Kinderlehrer and Stampacchia, 2000) characterizes the relation between a convex program and a VIP.

Lemma A.1. *Given a closed and convex set $\mathbb{Y} \subseteq \mathbb{R}^m$ and a continuously differentiable and convex function $f : \mathbb{Y} \rightarrow \mathbb{R}$, consider the optimization problem $\min_{\mathbf{y} \in \mathbb{Y}} f(\mathbf{y})$. Then $\mathbf{z}^* \in \mathbb{Y}$ is an optimal solution to this convex program if and only if $\langle \nabla f(\mathbf{y}^*), \mathbf{y} - \mathbf{y}^* \rangle \geq 0$ for all $\mathbf{y} \in \mathbb{Y}$.*

Based on Lemma A.1, we can then prove Proposition 5.4.

Proof of Proposition 5.4. First, we have $\mathbf{p}^{t+1} = h(\mathbf{p}^t; \mathbf{z})$ if and only if \mathbf{p}_w^{t+1} solves Equation (5.2) per Proposition 5.1. As the objective function in Equation (5.2), denoted as $f_w(\mathbf{p}_w) = r \cdot \langle c_w(\mathbf{p}^t; \mathbf{z}), \mathbf{p}_w \rangle + D\phi_w(\mathbf{p}_w, \mathbf{p}_w^t)$, is finite if and only if $\mathbf{p}_w \in \mathbb{Q}_w(\mathbf{p}_w^t)$, we may equivalently minimize $f_w(\mathbf{p}_w)$ over $\mathbb{Q}_w(\mathbf{p}_w^t)$, which is a closed set. Meanwhile, we have $\nabla f_w(\mathbf{p}_w) = r \cdot c_w(\mathbf{p}^t; \mathbf{z}) + \nabla \phi_w(\mathbf{p}_w) - \nabla \phi_w(\mathbf{p}_w^t)$ and $\nabla^2 f_w(\mathbf{p}_w) = \nabla^2 \phi_w(\mathbf{p}_w)$, which is positively definite as ϕ_w is strongly convex. Hence, $f_w(\mathbf{p}_w)$ is also strongly convex. The proof is then concluded by directly applying Lemma A.1. \square

A.2 Proof of Lemma 5.5

For any strategy $\mathbf{p} \in \mathbb{P}$, we define $\mathbb{K}_+(\mathbf{p}) = \text{supp}(\mathbf{p})$ and $\mathbb{K}_0(\mathbf{p}) = \mathbb{K} \setminus \text{supp}(\mathbf{p})$. Then for any $\mathbf{p}, \mathbf{p}' \in \mathbb{P}$, define $q_+(\mathbf{p}; \mathbf{p}')$ as a strategy with the k th element equal to p_k if $k \in \mathbb{K}_+(\mathbf{p}')$ and 0 otherwise. We also define $q_0(\mathbf{p}; \mathbf{p}') = \mathbf{p} - q_+(\mathbf{p}; \mathbf{p}')$.

Lemma A.2. *A feasible strategy $\mathbf{p}' \in \mathbb{P}^*(\mathbf{z})$ if and only if there exists $\mathbf{p}^* \in \mathbb{P}^*(\mathbf{z})$ such that*

$$\langle c(\mathbf{p}'; \mathbf{z}), \mathbf{p} - \mathbf{p}' \rangle \geq 0, \quad \forall \mathbf{p} \in \mathbb{Q}(\mathbf{p}^*). \quad (\text{A.1})$$

Proof. Denote the solution set to VIP (A.1) as $\mathbb{Q}^*(\mathbf{p}^*; \mathbf{z})$. We first prove that $\mathbb{Q}^*(\mathbf{p}^*; \mathbf{z}) \subseteq \mathbb{Q}(\mathbf{p}^*)$. If not so, then there must exist $\mathbf{p}'' \in \mathbb{Q}^*(\mathbf{p}^*; \mathbf{z})$ that is not covered by \mathbf{p}^* . Hence, some elements of $q_0(\mathbf{p}''; \mathbf{p}^*)$ must be positive, and

$$0 > \langle c(\mathbf{p}''; \mathbf{z}), -q_0(\mathbf{p}''; \mathbf{p}^*) \rangle = \langle c(\mathbf{p}''; \mathbf{z}), q_+(\mathbf{p}''; \mathbf{p}^*) - \mathbf{p}'' \rangle \geq 0, \quad (\text{A.2})$$

which is a contradiction. The last inequality holds because $q_+(\mathbf{p}''; \mathbf{p}^*)$ is covered by \mathbf{p}^* . Since both \mathbf{p}' and \mathbf{p} must be covered by \mathbf{p}^* , $\mathbb{Q}^*(\mathbf{p}^*; \mathbf{z})$ can be viewed as the solution set of a routing game with a restricted feasible set $\mathbb{K}_+(\mathbf{p}^*)$. As $\mathbf{p}^* \in \mathbb{P}^*(\mathbf{z}) \cap \mathbb{Q}(\mathbf{p}^*)$, we have $\mathbf{p}^* \in \mathbb{Q}^*(\mathbf{p}^*; \mathbf{z})$. Because both \mathbf{p}' and \mathbf{p}^* belong to $\mathbb{Q}^*(\mathbf{p}^*; \mathbf{z})$, Proposition 4.4 then implies that $\Lambda \mathbf{q} \circ \mathbf{p}' = \Lambda \mathbf{q} \circ \mathbf{p}^*$, and accordingly $\mathbf{p}' \in \mathbb{P}^*(\mathbf{z})$. \square

Now we are ready to prove Lemma 5.5.

Proof of Lemma 5.5. By replacing both \mathbf{p}^t and \mathbf{p}^{t+1} by $\hat{\mathbf{p}}$ in Equation (5.4) (see Proposition 5.4), and summarizing over $w \in \mathbb{W}$, we arrive at the following: $\hat{\mathbf{p}} \in \mathbb{P}$ satisfies $\hat{\mathbf{p}} = h(\hat{\mathbf{p}}; \mathbf{z})$ if and only if

$$\langle c(\hat{\mathbf{p}}; \mathbf{z}), \mathbf{p} - \hat{\mathbf{p}} \rangle \geq 0, \quad \forall \mathbf{p} \in \mathbb{Q}(\hat{\mathbf{p}}), \quad (\text{A.3})$$

If $\mathbf{p}^* \in \mathbb{P}^*(\mathbf{z})$, then $\langle c(\mathbf{p}^*; \mathbf{z}), \mathbf{p} - \mathbf{p}^* \rangle \geq 0$ for all $\mathbf{p} \in \mathbb{P}$. As $\mathbb{Q}(\hat{\mathbf{p}}) \subseteq \mathbb{P}$, Equation (A.3) must hold, which implies $\hat{\mathbf{p}} = h(\hat{\mathbf{p}}; \mathbf{z})$. Conversely, if $\hat{\mathbf{p}} = h(\hat{\mathbf{p}}; \mathbf{z})$ and $\mathbf{p}^* \in \mathbb{Q}(\hat{\mathbf{p}})$ for some $\mathbf{p}^* \in \mathbb{P}^*(\mathbf{z})$, then VIP (A.3) still holds when we replace $\mathbb{Q}(\hat{\mathbf{p}})$ with $\mathbb{Q}(\mathbf{p}^*)$ since $\mathbb{Q}(\mathbf{p}^*) \subseteq \mathbb{Q}(\hat{\mathbf{p}})$. Invoking Lemma A.2 then proves $\hat{\mathbf{p}}$ is a WE. \square

A.3 Proof of Theorem 5.7

We first provide several lemmas that will be used in the proof. In all of these lemmas, we assume that \mathbb{X} is a closed convex set.

Lemma A.3 (Chen and Teboulle (1993)). *For any Bregman divergence $D_\phi : \mathbb{X} \times \mathbb{X} \rightarrow \mathbb{R} \cup \{\infty\}$ and any $\mathbf{x}, \mathbf{x}', \mathbf{x}'' \in \mathbb{X}$, we have*

$$D_\phi(\mathbf{x}, \mathbf{x}') + D_\phi(\mathbf{x}', \mathbf{x}'') - D_\phi(\mathbf{x}, \mathbf{x}'') = \langle \mathbf{x} - \mathbf{x}', \nabla \phi(\mathbf{x}'') - \nabla \phi(\mathbf{x}') \rangle. \quad (\text{A.4})$$

Lemma A.4. *If ϕ is σ -strongly convex with respect to $\|\cdot\|$ on \mathbb{X} , then for all $\mathbf{x}, \mathbf{x}' \in \mathbb{X}$, the induced Bregman divergence $D_\phi(\mathbf{x}, \mathbf{x}')$ satisfies $D_\phi(\mathbf{x}, \mathbf{x}') \geq \sigma/2 \cdot \|\mathbf{x} - \mathbf{x}'\|^2$.*

Proof. By the definition of Bregman divergence, $D_\phi(\mathbf{x}, \mathbf{x}') = \phi(\mathbf{x}) - \phi(\mathbf{x}') - \langle \nabla \phi(\mathbf{x}'), \mathbf{x} - \mathbf{x}' \rangle$. By the definition of strong convexity, $\phi(\mathbf{x}) \geq \phi(\mathbf{x}') + \langle \nabla \phi(\mathbf{x}'), \mathbf{x} - \mathbf{x}' \rangle + \sigma/2 \cdot \|\mathbf{x} - \mathbf{x}'\|^2$. \square

Lemma A.5 (Beck and Teboulle (2003)). *The negative entropy function $\phi(\mathbf{x}) = \langle \mathbf{x}, \log(\mathbf{x}) \rangle$, which induces the KL divergence, is 1-strongly convex with respect to ℓ_1 norm $\|\cdot\|_1$.*

Lemma A.6. *For all $\mathbf{x} \in \mathbb{X}$, we have $\|\mathbf{x}\|_2 \leq \|\mathbf{x}\|_1$.*

Proof. It is a direct corollary of the Cauchy-Schwartz inequality. \square

Lemma A.7 (Marcotte and Wu (1995)). *For any two vectors $\mathbf{x}, \mathbf{x}' \in \mathbb{X}$, we have $\langle \mathbf{x}, \mathbf{x}' \rangle - \|\mathbf{x}'\|_2^2 \leq \frac{1}{4} \cdot \|\mathbf{x}\|_2^2$.*

Now we are ready to prove Theorem 5.7.

Proof of Theorem 5.7. For all $\mathbf{p}^* \in \mathbb{P}^*(\mathbf{z})$, Lemma A.3 first implies that

$$D_{\phi_w}(\mathbf{p}_w^*, \mathbf{p}_w^{t+1}) = D_{\phi_w}(\mathbf{p}_w^*, \mathbf{p}_w^t) - D_{\phi_w}(\mathbf{p}_w^{t+1}, \mathbf{p}_w^t) + \langle \nabla \phi(\mathbf{p}_w^t) - \nabla \phi(\mathbf{p}_w^{t+1}), \mathbf{p}_w^* - \mathbf{p}_w^{t+1} \rangle \quad (\text{A.5})$$

Combining Equation (5.4) in Lemma 5.4 and Equation (A.5), we arrive at

$$D_{\phi_w}(\mathbf{p}_w^*, \mathbf{p}_w^t) - D_{\phi_w}(\mathbf{p}_w^*, \mathbf{p}_w^{t+1}) \geq D_{\phi_w}(\mathbf{p}_w^{t+1}, \mathbf{p}_w^t) + r \cdot \langle c_w(\mathbf{p}^t; \mathbf{z}), \mathbf{p}_w^{t+1} - \mathbf{p}_w^* \rangle. \quad (\text{A.6})$$

Summarizing Equation (A.6) for all $w \in \mathbb{W}$ leads to

$$\begin{aligned} \tilde{D}_\phi(\mathbf{p}^*, \mathbf{p}^t) - \tilde{D}_\phi(\mathbf{p}^*, \mathbf{p}^{t+1}) &\geq \tilde{D}_\phi(\mathbf{p}^t, \mathbf{p}^{t+1}) + r \cdot \langle c(\mathbf{p}^t; \mathbf{z}), \mathbf{p}^{t+1} - \mathbf{p}^* \rangle \\ &\geq \tilde{D}_\phi(\mathbf{p}^t, \mathbf{p}^{t+1}) + r \cdot \langle c(\mathbf{p}^t; \mathbf{z}) - c(\mathbf{p}^*; \mathbf{z}), \mathbf{p}^{t+1} - \mathbf{p}^* \rangle, \end{aligned} \quad (\text{A.7})$$

where the second inequality holds because $\langle c(\mathbf{p}^*; \mathbf{z}), \mathbf{p}^{t+1} - \mathbf{p}^* \rangle \geq 0$. Below we further bound the two terms on the right-hand side of Equation (A.7). First,

$$\tilde{D}_\phi(\mathbf{p}^{t+1}, \mathbf{p}^t) \geq \frac{1}{2} \cdot \sum_{w \in \mathbb{W}} \|\mathbf{p}_w^t - \mathbf{p}_w^{t+1}\|_1^2 \geq \sum_{w \in \mathbb{W}} \|\mathbf{p}_w^t - \mathbf{p}_w^{t+1}\|_2^2 = \frac{1}{2} \cdot \|\mathbf{p}^t - \mathbf{p}^{t+1}\|_2^2, \quad (\text{A.8})$$

where the first inequality follows from Lemmas A.4 and A.5, and the second follows from Lemma A.6. Second,

$$\begin{aligned} \langle c(\mathbf{p}^t; \mathbf{z}) - c(\mathbf{p}^*; \mathbf{z}), \mathbf{p}^{t+1} - \mathbf{p}^* \rangle &= \langle c(\mathbf{p}^t; \mathbf{z}) - c(\mathbf{p}^*; \mathbf{z}), \mathbf{p}^{t+1} - \mathbf{p}^t + \mathbf{p}^t - \mathbf{p}^* \rangle \\ &\geq \langle c(\mathbf{p}^t; \mathbf{z}) - c(\mathbf{p}^*; \mathbf{z}), \mathbf{p}^{t+1} - \mathbf{p}^t \rangle + c_z \cdot \|c(\mathbf{p}^t; \mathbf{z}) - c(\mathbf{p}^*; \mathbf{z})\|_2^2 \geq -\frac{1}{4c_z} \cdot \|\mathbf{p}^t - \mathbf{p}^{t+1}\|_2^2, \end{aligned} \quad (\text{A.9})$$

where the first inequality is guaranteed by the cocoercivity of $c(\mathbf{p}; \mathbf{z})$ and the second follows from Lemma A.7. Plugging Equations (A.8) and (A.9) into Equation (A.7) results in

$$D_\phi(\mathbf{p}^*, \mathbf{p}^t) - D_\phi(\mathbf{p}^*, \mathbf{p}^{t+1}) \geq \frac{2c_z - r}{4c_z} \cdot \|\mathbf{p}^t - \mathbf{p}^{t+1}\|_2^2. \quad (\text{A.10})$$

For a \mathbf{p}^* covered by \mathbf{p}^0 per the initial condition, $\tilde{D}_\phi(\mathbf{p}^*, \mathbf{p}^0) < \infty$ per Lemma 5.3. For such \mathbf{p}^* , the divergence $\tilde{D}_\phi(\mathbf{p}^*, \mathbf{p}^t)$ is monotonically decreasing as long as $r < 2c_z$ according to Equation (A.10). Thus, the limit of $D_\phi(\mathbf{p}^*, \mathbf{p}^t)$ exists according to the monotone convergence theorem. Hence, by letting $t \rightarrow \infty$ on both sides of Equation (A.10), the squeeze theorem ensures $\|\mathbf{p}^t - \mathbf{p}^{t+1}\|_2 \rightarrow 0$.

We should note the existence of $\lim_{t \rightarrow \infty} \tilde{D}_\phi(\mathbf{p}^*, \mathbf{p}^t)$ for some \mathbf{p}^* does not imply the limit must be zero. Nor does it ensure the convergence of $\{\mathbf{p}_t\}$. However, since \mathbb{P} is compact, the Bolzano-Weierstrass theorem guarantees the sequence $\{\mathbf{p}^t\}$ must have a convergent subsequence $\{\mathbf{p}^{t_j}\}$. Denote $\hat{\mathbf{p}}$ as the limit of \mathbf{p}^{t_j} when $j \rightarrow \infty$. Assume $\|h(\hat{\mathbf{p}}; \mathbf{z}) - \hat{\mathbf{p}}\| = \delta$ for some $\delta > 0$. That is, the limit of the subsequence $\hat{\mathbf{p}}$ is not a fixed point of the ILD. We proceed to establish a contradiction. Note that

$$\begin{aligned} \|\mathbf{p}^{t_j+1} - \mathbf{p}^{t_j}\|_2 &= \|h(\mathbf{p}^{t_j}; \mathbf{z}) - \mathbf{p}^{t_j}\|_2 = \|h(\mathbf{p}^{t_j}; \mathbf{z}) - h(\hat{\mathbf{p}}; \mathbf{z}) + h(\hat{\mathbf{p}}; \mathbf{z}) - \hat{\mathbf{p}} + \hat{\mathbf{p}} - \mathbf{p}^{t_j}\|_2 \\ &\geq \|h(\hat{\mathbf{p}}; \mathbf{z}) - \hat{\mathbf{p}}\|_2 - \|h(\mathbf{p}^{t_j}; \mathbf{z}) - h(\hat{\mathbf{p}}; \mathbf{z}) + \hat{\mathbf{p}} - \mathbf{p}^{t_j}\|_2 \geq \delta - \|h(\mathbf{p}^{t_j}; \mathbf{z}) - h(\hat{\mathbf{p}}; \mathbf{z})\|_2 - \|\hat{\mathbf{p}} - \mathbf{p}^{t_j}\|_2. \end{aligned} \quad (\text{A.11})$$

Letting $j \rightarrow \infty$ on both sides of Equation (A.11), the left-hand side then converges to 0. Meanwhile, on the right-hand side, we also have $\|\hat{\mathbf{p}} - \mathbf{p}^{t_j}\| \rightarrow 0$ and thus $\|h(\mathbf{p}^{t_j}; \mathbf{z}) - h(\hat{\mathbf{p}}; \mathbf{z})\| \rightarrow 0$ due to the continuity of $h(\mathbf{p}; \mathbf{z})$ with respect to \mathbf{p} . We then have $0 = \|h(\mathbf{p}^{t_j}; \mathbf{z}) - \mathbf{p}^{t_j}\|_2 \geq \delta > 0$, a contradiction. Thus, $\hat{\mathbf{p}} = h(\hat{\mathbf{p}}; \mathbf{z})$.

We next claim $\mathbf{p}^* \in \mathbb{Q}(\mathbf{p}^0)$ implies $\mathbf{p}^* \in \mathbb{Q}(\hat{\mathbf{p}})$. Otherwise, $D_\phi(\mathbf{p}^*, \hat{\mathbf{p}})$ would be unbounded, which is impossible given $D_\phi(\mathbf{p}^*, \mathbf{p}^t)$ is monotonically decreasing. This, along with the fact that $\hat{\mathbf{p}}$ is a fixed point of ILD, allows us to invoke Lemma 5.5 to show the limit $\hat{\mathbf{p}}$ is indeed a WE.

To recapitulate, we have established (i) $\mathbf{p}^{t_j} \rightarrow \hat{\mathbf{p}}$ when $j \rightarrow \infty$; (ii) $\hat{\mathbf{p}} \in \mathbb{P}^*(\mathbf{z})$; and (iii) the limit of $\tilde{D}_\phi(\hat{\mathbf{p}}, \mathbf{p}^t)$ exists. Combining all three, we conclude $\tilde{D}_\phi(\hat{\mathbf{p}}, \mathbf{p}^t) \rightarrow 0$ when $t \rightarrow \infty$, which implies $\mathbf{p}^t \rightarrow \hat{\mathbf{p}}$.

□

Acknowledgements

This research is funded by US National Science Foundation’s Civil Infrastructure System (CIS) Program under the award CMMI # 2225087 and Energy, Power, Control, and Networks (EPCN) Program under the award ECCS # 2048075.

References

- Abadi, M., Agarwal, A., Barham, P., Brevdo, E., Chen, Z., Citro, C., Corrado, G. S., Davis, A., Dean, J., Devin, M., et al. (2016). Tensorflow: Large-scale machine learning on heterogeneous distributed systems. *arXiv preprint arXiv:1603.04467*.
- Abdulaal, M. and LeBlanc, L. J. (1979). Continuous equilibrium network design models. *Transportation Research Part B: Methodological*, 13(1):19–32.
- Agrawal, A., Amos, B., Barratt, S., Boyd, S., Diamond, S., and Kolter, J. Z. (2019). Differentiable convex optimization layers. In *Advances in Neural Information Processing Systems*, pages 9558–9570.
- Aiyoshi, E. and Shimizu, K. (1984). A solution method for the static constrained stackelberg problem via penalty method. *IEEE Transactions on Automatic Control*, 29(12):1111–1114.
- Al-Khayyal, F. A., Horst, R., and Pardalos, P. M. (1992). Global optimization of concave functions subject to quadratic constraints: an application in nonlinear bilevel programming. *Annals of Operations Research*, 34(1):125–147.
- Al-Rfou, R., Alain, G., Almahairi, A., Angermueller, C., Bahdanau, D., Ballas, N., Bastien, F., Bayer, J., Belikov, A., Belopolsky, A., et al. (2016). Theano: A python framework for fast computation of mathematical expressions. *arXiv e-prints*, pages arXiv-1605.
- Amos, B. and Kolter, J. Z. (2017). Optnet: Differentiable optimization as a layer in neural networks. In *Proceedings of the 34th International Conference on Machine Learning*, pages 136–145.
- Bahrami, S. and Roorda, M. J. (2020). Optimal traffic management policies for mixed human and automated traffic flows. *Transportation Research Part A: Policy and Practice*, 135:130–143.
- Bar-Gera, H. and Luzon, A. (2007). Non-unique route flow solutions for user-equilibrium assignments. *Traffic Engineering & Control*, 48(9).
- Bard, J. F. (1988). Convex two-level optimization. *Mathematical programming*, 40(1):15–27.
- Bard, J. F. and Falk, J. E. (1982). An explicit solution to the multi-level programming problem. *Computers & Operations Research*, 9(1):77–100.
- Baydin, A. G., Pearlmutter, B. A., Radul, A. A., and Siskind, J. M. (2018). Automatic differentiation in machine learning: a survey. *Journal of machine learning research*, 18.
- Beck, A. and Teboulle, M. (2003). Mirror descent and nonlinear projected subgradient methods for convex optimization. *Operations Research Letters*, 31(3):167–175.
- Beckmann, M., McGuire, C. B., and Winsten, C. B. (1956). Studies in the economics of transportation. *The Economic Journal*, 67(265):116–118.
- Ben-Akiva, M. E., Lerman, S. R., and Lerman, S. R. (1985). *Discrete choice analysis: theory and application to travel demand*, volume 9. MIT press.

- Bertsekas, D. P. and Gafni, E. M. (1982). Projection methods for variational inequalities with application to the traffic assignment problem. In *Nondifferential and variational techniques in optimization*, pages 139–159. Springer.
- Bialas, W., Karwan, M., and Shaw, J. (1980). A parametric complementary pivot approach for two-level linear programming. *State University of New York at Buffalo*, 57.
- Bialas, W. F. and Karwan, M. H. (1984). Two-level linear programming. *Management science*, 30(8):1004–1020.
- Bıyık, E., Lazar, D. A., Pedarsani, R., and Sadigh, D. (2018). Altruistic autonomy: Beating congestion on shared roads. In *International Workshop on the Algorithmic Foundations of Robotics*, pages 887–904. Springer.
- Björnerstedt, J. and Weibull, J. W. (1994). Nash equilibrium and evolution by imitation. Technical report, IUI Working Paper.
- Boyce, D. and Xie, J. (2013). Assigning user class link flows uniquely. *Transportation Research Part A: Policy and Practice*, 53:22–35.
- Braess, D. (1968). Über ein paradoxon aus der verkehrsplanung. *Unternehmensforschung*, 12(1):258–268.
- Candler, W. and Townsley, R. (1982). A linear two-level programming problem. *Computers & Operations Research*, 9(1):59–76.
- Cantarella, G. and Sforza, A. (1987). Methods for equilibrium network traffic signal setting. In *Flow Control of Congested Networks*, pages 69–89. Springer.
- Cascetta, E. and Cantarella, G. E. (1991). A day-to-day and within-day dynamic stochastic assignment model. *Transportation Research Part A: General*, 25(5):277–291.
- Chen, G. and Teboulle, M. (1993). Convergence analysis of a proximal-like minimization algorithm using bregman functions. *SIAM Journal on Optimization*, 3(3):538–543.
- Chen, Z., He, F., Yin, Y., and Du, Y. (2017). Optimal design of autonomous vehicle zones in transportation networks. *Transportation Research Part B: Methodological*, 99:44–61.
- Chen, Z., He, F., Zhang, L., and Yin, Y. (2016). Optimal deployment of autonomous vehicle lanes with endogenous market penetration. *Transportation Research Part C: Emerging Technologies*, 72:143–156.
- Chen, Z., Lin, X., Yin, Y., and Li, M. (2020). Path controlling of automated vehicles for system optimum on transportation networks with heterogeneous traffic stream. *Transportation Research Part C: Emerging Technologies*, 110:312–329.
- Colson, B., Marcotte, P., and Savard, G. (2007). An overview of bilevel optimization. *Annals of operations research*, 153(1):235–256.
- Cournot, A. A. (1897). *Researches into the Mathematical Principles of the Theory of Wealth*. Macmillan.
- Dafermos, S. (1980). Traffic equilibrium and variational inequalities. *Transportation Science*, 14(1):42–54.
- Dafermos, S. (1983). An iterative scheme for variational inequalities. *Mathematical Programming*, 26(1):40–47.
- Dafermos, S. (1988). Sensitivity analysis in variational inequalities. *Mathematics of Operations Research*, 13(3):421–434.
- Dafermos, S. C. (1973). Toll patterns for multiclass-user transportation networks. *Transportation science*, 7(3):211–223.

- Dantzig, G. B., Harvey, R. P., Lansdowne, Z. F., Robinson, D. W., and Maier, S. F. (1979). Formulating and solving the network design problem by decomposition. *Transportation Research Part B: Methodological*, 13(1):5–17.
- Delle Site, P. (2021). Pricing of connected and autonomous vehicles in mixed-traffic networks. *Transportation Research Record*.
- Diamond, S. and Boyd, S. (2016). Cvxpy: A python-embedded modeling language for convex optimization. *The Journal of Machine Learning Research*, 17(1):2909–2913.
- Doan, T. T., Bose, S., Nguyen, D. H., and Beck, C. L. (2018). Convergence of the iterates in mirror descent methods. *IEEE control systems letters*, 3(1):114–119.
- Eash, R., Chon, K., Lee, Y., and Boyce, D. (1979). Equilibrium traffic assignment on an aggregated highway network for sketch planning. *Transportation Research*, 13:243–257.
- Feng, L., Xie, J., Nie, Y., and Liu, X. (2020). Efficient algorithm for the traffic assignment problem with side constraints. *Transportation research record*, 2674(4):129–139.
- Finn, C., Abbeel, P., and Levine, S. (2017). Model-agnostic meta-learning for fast adaptation of deep networks. In *International Conference on Machine Learning*, pages 1126–1135. PMLR.
- Fisk, C. (1984). Game theory and transportation systems modelling. *Transportation Research Part B: Methodological*, 18(4-5):301–313.
- Fisk, C. S. (1986). A conceptual framework for optimal transportation systems planning with integrated supply and demand models. *Transportation Science*, 20(1):37–47.
- Florian, M. and Nguyen, S. (1976). An application and validation of equilibrium trip assignment methods. *Transportation Science*, 10(4):374–390.
- Franceschi, L., Donini, M., Frasconi, P., and Pontil, M. (2017). Forward and reverse gradient-based hyperparameter optimization. In *International Conference on Machine Learning*, pages 1165–1173. PMLR.
- Franceschi, L., Frasconi, P., Salzo, S., Grazzi, R., and Pontil, M. (2018). Bilevel programming for hyperparameter optimization and meta-learning. In *International Conference on Machine Learning*, pages 1568–1577. PMLR.
- Frank, M. and Wolfe, P. (1956). An algorithm for quadratic programming. *Naval research logistics quarterly*, 3(1-2):95–110.
- Friesz, T. L., Bernstein, D., and Kydes, N. (2004). Dynamic congestion pricing in disequilibrium. *Networks and Spatial Economics*, 4(2):181–202.
- Friesz, T. L., Bernstein, D., Mehta, N. J., Tobin, R. L., and Ganjalizadeh, S. (1994). Day-to-day dynamic network disequilibria and idealized traveler information systems. *Operations Research*, 42(6):1120–1136.
- Friesz, T. L. and Harker, P. T. (1985). Properties of the iterative optimization-equilibrium algorithm. *Civil Engineering Systems*, 2(3):142–154.
- Friesz, T. L., Tobin, R. L., Cho, H.-J., and Mehta, N. J. (1990). Sensitivity analysis based heuristic algorithms for mathematical programs with variational inequality constraints. *Mathematical Programming*, 48(1-3):265–284.
- Frostig, R., Johnson, M. J., and Leary, C. (2018). Compiling machine learning programs via high-level tracing. *Systems for Machine Learning*, pages 23–24.

- Gartner, N. H. (1985). Demand-responsive traffic signal control research. *Transportation Research Part A: General*, 19(5-6):369–373.
- Goodfellow, I., Bengio, Y., Courville, A., and Bengio, Y. (2016). *Deep learning*, volume 1. MIT Press.
- Grazzi, R., Franceschi, L., Pontil, M., and Salzo, S. (2020). On the iteration complexity of hypergradient computation. In *International Conference on Machine Learning*, pages 3748–3758. PMLR.
- Griewank, A. et al. (1989). On automatic differentiation. *Mathematical Programming: recent developments and applications*, 6(6):83–107.
- Han, L. and Du, L. (2012). On a link-based day-to-day traffic assignment model. *Transportation Research Part B: Methodological*, 46(1):72–84.
- Harker, P. T. (1988). Multiple equilibrium behaviors on networks. *Transportation science*, 22(1):39–46.
- Harsanyi, J. C., Selten, R., et al. (1988). A general theory of equilibrium selection in games. *MIT Press Books*, 1.
- Hu, Y., Anderson, L., Li, T.-M., Sun, Q., Carr, N., Ragan-Kelley, J., and Durand, F. (2019). DiffTaichi: Differentiable programming for physical simulation. *arXiv preprint arXiv:1910.00935*.
- Improta, G. (1987). Mathematical programming methods for urban network control. In *Flow control of congested networks*, pages 35–68. Springer.
- Ishizuka, Y. and Aiyoshi, E. (1992). Double penalty method for bilevel optimization problems. *Annals of Operations Research*, 34(1):73–88.
- Jin, W., Wang, Z., Yang, Z., and Mou, S. (2020). Pontryagin differentiable programming: An end-to-end learning and control framework. *Advances in Neural Information Processing Systems*, 33:7979–7992.
- Kinderlehrer, D. and Stampacchia, G. (2000). *An introduction to variational inequalities and their applications*. SIAM.
- Krichene, W., Krichene, S., and Bayen, A. (2015). Convergence of mirror descent dynamics in the routing game. In *2015 European Control Conference (ECC)*, pages 569–574. IEEE.
- Kullback, S. (1997). *Information theory and statistics*. Courier Corporation.
- Lawphongpanich, S. and Hearn, D. W. (2004). An mpec approach to second-best toll pricing. *Mathematical programming*, 101(1):33–55.
- Lazar, D. A., Coogan, S., and Pedarsani, R. (2019). Optimal tolling for heterogeneous traffic networks with mixed autonomy. In *2019 IEEE 58th Conference on Decision and Control (CDC)*, pages 4103–4108. IEEE.
- Leblanc, L. J. (1975). An algorithm for the discrete network design problem. *Transportation Science*, 9(3):183–199.
- LeBlanc, L. J., Morlok, E. K., and Pierskalla, W. P. (1975). An efficient approach to solving the road network equilibrium traffic assignment problem. *Transportation research*, 9(5):309–318.
- LeCun, Y., Bengio, Y., and Hinton, G. (2015). Deep learning. *nature*, 521(7553):436–444.
- LeCun, Y., Bottou, L., Orr, G. B., and Müller, K.-R. (1996). Efficient backprop. In *Neural Networks: Tricks of the Trade*.
- Levin, M. W. and Boyles, S. D. (2016). A cell transmission model for dynamic lane reversal with autonomous vehicles. *Transportation Research Part C: Emerging Technologies*, 68:126–143.

- Li, C., Yang, H., Zhu, D., and Meng, Q. (2012). A global optimization method for continuous network design problems. *Transportation Research Part B: Methodological*, 46(9):1144–1158.
- Li, J., Yu, J., Nie, Y. M., and Wang, Z. (2020). End-to-end learning and intervention in games. *Advances in Neural Information Processing Systems*, 33.
- Li, R., Liu, X., and Nie, Y. M. (2018). Managing partially automated network traffic flow: Efficiency vs. stability. *Transportation Research Part B: Methodological*, 114:300–324.
- Li, W., Kockelman, K. M., and Huang, Y. (2021). Traffic and welfare impacts of credit-based congestion pricing applications: An austin case study. *Transportation Research Record*, 2675(1):10–24.
- Linnainmaa, S. (1970). The representation of the cumulative rounding error of an algorithm as a taylor expansion of the local rounding errors. *Master’s Thesis (in Finnish), Univ. Helsinki*, pages 6–7.
- Liu, H., Simonyan, K., and Yang, Y. (2018). Darts: Differentiable architecture search. *arXiv preprint arXiv:1806.09055*.
- Liu, R., Gao, J., Zhang, J., Meng, D., and Lin, Z. (2021). Investigating bi-level optimization for learning and vision from a unified perspective: A survey and beyond. *IEEE Transactions on Pattern Analysis and Machine Intelligence*.
- Loridan, P. and Morgan, J. (1996). Weak via strong stackelberg problem: new results. *Journal of global Optimization*, 8(3):263–287.
- Lu, G., Nie, Y. M., Liu, X., and Li, D. (2019). Trajectory-based traffic management inside an autonomous vehicle zone. *Transportation Research Part B: Methodological*, 120:76–98.
- Luketina, J., Berglund, M., Greff, K., and Raiko, T. (2016). Scalable gradient-based tuning of continuous regularization hyperparameters. In *International conference on machine learning*, pages 2952–2960. PMLR.
- Luo, Z.-Q., Pang, J.-S., and Ralph, D. (1996). *Mathematical programs with equilibrium constraints*. Cambridge University Press.
- Maclaurin, D., Duvenaud, D., and Adams, R. (2015). Gradient-based hyperparameter optimization through reversible learning. In *International conference on machine learning*, pages 2113–2122. PMLR.
- Mahmassani, H. S. (2016). 50th anniversary invited article—autonomous vehicles and connected vehicle systems: Flow and operations considerations. *Transportation Science*, 50(4):1140–1162.
- Marcotte, P. (1983). Network optimization with continuous control parameters. *Transportation Science*, 17(2):181–197.
- Marcotte, P. (1986). Network design problem with congestion effects: A case of bilevel programming. *Mathematical programming*, 34(2):142–162.
- Marcotte, P. and Marquis, G. (1992). Efficient implementation of heuristics for the continuous network design problem. *Annals of Operations Research*, 34(1):163–176.
- Marcotte, P. and Wu, J. H. (1995). On the convergence of projection methods: application to the decomposition of affine variational inequalities. *Journal of Optimization Theory and Applications*, 85(2):347–362.
- McFadden, D. (1973). Conditional logit analysis of qualitative choice behavior. *Frontiers in Econometrics*, pages 105–142.
- Mehr, N. and Horowitz, R. (2019). Pricing traffic networks with mixed vehicle autonomy. In *2019 American Control Conference (ACC)*, pages 2676–2682. IEEE.

- Meng, Q., Yang, H., and Bell, M. G. (2001). An equivalent continuously differentiable model and a locally convergent algorithm for the continuous network design problem. *Transportation Research Part B: Methodological*, 35(1):83–105.
- Mertikopoulos, P. and Zhou, Z. (2019). Learning in games with continuous action sets and unknown payoff functions. *Mathematical Programming*, 173(1-2):465–507.
- Metz, L., Poole, B., Pfau, D., and Sohl-Dickstein, J. (2016). Unrolled generative adversarial networks. *arXiv preprint arXiv:1611.02163*.
- Migdalas, A. (1995). Bilevel programming in traffic planning: Models, methods and challenge. *Journal of Global Optimization*, 7(4):381–405.
- Nagurney, A. (2013). *Network economics: A variational inequality approach*, volume 10. Springer Science & Business Media.
- Nemirovskij, A. S. and Yudin, D. B. (1983). *Problem complexity and method efficiency in optimization*. Wiley-Interscience.
- Nesterov, Y. (2009). Primal-dual subgradient methods for convex problems. *Mathematical programming*, 120(1):221–259.
- Paszke, A., Gross, S., Massa, F., Lerer, A., Bradbury, J., Chanan, G., Killeen, T., Lin, Z., Gimelshein, N., Antiga, L., et al. (2019). Pytorch: An imperative style, high-performance deep learning library. *Advances in neural information processing systems*, 32.
- Patriksson, M. and Rockafellar, R. T. (2002). A mathematical model and descent algorithm for bilevel traffic management. *Transportation Science*, 36(3):271–291.
- Peeta, S. and Mahmassani, H. S. (1995). Multiple user classes real-time traffic assignment for online operations: a rolling horizon solution framework. *Transportation Research Part C: Emerging Technologies*, 3(2):83–98.
- Poorzahedy, H. and Turnquist, M. A. (1982). Approximate algorithms for the discrete network design problem. *Transportation Research Part B: Methodological*, 16(1):45–55.
- Rademacher, H. (1919). Über partielle und totale differenzierbarkeit von funktionen mehrerer variablen und über die transformation der doppelintegrale. *Mathematische Annalen*, 79(4):340–359.
- Radhakrishnan, A., Belkin, M., and Uhler, C. (2020). Linear convergence of generalized mirror descent with time-dependent mirrors. *arXiv preprint arXiv:2009.08574*.
- Roughgarden, T. and Tardos, É. (2002). How bad is selfish routing? *Journal of the ACM*, 49(2):236–259.
- Rumelhart, D. E., Hinton, G. E., and Williams, R. J. (1986). Learning representations by back-propagating errors. *nature*, 323(6088):533–536.
- Sandholm, W. H. (2015). Population games and deterministic evolutionary dynamics. In *Handbook of game theory with economic applications*, volume 4, pages 703–778. Elsevier.
- Scutari, G., Palomar, D. P., Facchinei, F., and Pang, J.-S. (2010). Convex optimization, game theory, and variational inequality theory. *IEEE Signal Processing Magazine*, 27(3):35–49.
- Shaban, A., Cheng, C.-A., Hatch, N., and Boots, B. (2019). Truncated back-propagation for bilevel optimization. In *The 22nd International Conference on Artificial Intelligence and Statistics*, pages 1723–1732. PMLR.
- Sharon, G., Albert, M., Rambha, T., Boyles, S., and Stone, P. (2018). Traffic optimization for a mixture of

- self-interested and compliant agents. In *Proceedings of the AAAI Conference on Artificial Intelligence*, volume 32.
- Sheffi, Y. (1985). *Urban transportation networks*, volume 6. Prentice-Hall, Englewood Cliffs, NJ.
- Sherali, H. D., Soyster, A. L., and Murphy, F. H. (1983). Stackelberg-nash-cournot equilibria: characterizations and computations. *Operations Research*, 31(2):253–276.
- Simoni, M. D., Kockelman, K. M., Gurumurthy, K. M., and Bischoff, J. (2019). Congestion pricing in a world of self-driving vehicles: An analysis of different strategies in alternative future scenarios. *Transportation Research Part C: Emerging Technologies*, 98:167–185.
- Smith, J. M. (1979a). Game theory and the evolution of behaviour. *Proceedings of the Royal Society of London. Series B. Biological Sciences*, 205(1161):475–488.
- Smith, M. (1979b). The marginal cost taxation of a transportation network. *Transportation Research Part B: Methodological*, 13(3):237–242.
- Smith, M. (1979c). Traffic control and route-choice; a simple example. *Transportation Research Part B: Methodological*, 13(4):289–294.
- Smith, M. and Mounce, R. (2011). A splitting rate model of traffic re-routeing and traffic control. *Procedia-Social and Behavioral Sciences*, 17:316–340.
- Smith, M. and Van Vuren, T. (1993). Traffic equilibrium with responsive traffic control. *Transportation science*, 27(2):118–132.
- Smith, M. and Wisten, M. (1995). A continuous day-to-day traffic assignment model and the existence of a continuous dynamic user equilibrium. *Annals of Operations Research*, 60(1):59–79.
- Smith, M. J. (1984). The stability of a dynamic model of traffic assignment—an application of a method of lyapunov. *Transportation science*, 18(3):245–252.
- Speelpenning, B. (1980). *Compiling fast partial derivatives of functions given by algorithms*. PhD thesis, University of Illinois at Urbana-Champaign.
- Suwansirikul, C., Friesz, T. L., and Tobin, R. L. (1987). Equilibrium decomposed optimization: a heuristic for the continuous equilibrium network design problem. *Transportation science*, 21(4):254–263.
- Talebpour, A., Mahmassani, H. S., and Elfar, A. (2017). Investigating the effects of reserved lanes for autonomous vehicles on congestion and travel time reliability. *Transportation Research Record*, 2622(1):1–12.
- Tan, H.-N., Gershwin, S. B., and Athans, M. (1979). Hybrid optimization in urban traffic networks. Technical report, Massachusetts Institute of Technology.
- Tian, Y., Shen, L., Su, G., Li, Z., and Liu, W. (2020). Alphagan: Fully differentiable architecture search for generative adversarial networks. *arXiv preprint arXiv:2006.09134*.
- Tobin, R. L. (1986). Sensitivity analysis for variational inequalities. *Journal of Optimization Theory and Applications*, 48(1):191–204.
- Tobin, R. L. and Friesz, T. L. (1988). Sensitivity analysis for equilibrium network flow. *Transportation Science*, 22(4):242–250.
- Van Vuren, T. and Watling, D. (1991). A multiple user class assignment model for route guidance. *Transportation research record*, pages 22–22.
- Verhoef, E. T. (2002). Second-best congestion pricing in general networks. heuristic algorithms for finding

- second-best optimal toll levels and toll points. *Transportation Research Part B: Methodological*, 36(8):707–729.
- Vickrey, W. S. (1969). Congestion theory and transport investment. *The American Economic Review*, 59(2):251–260.
- von Stackelberg, H. (1952). *The theory of the market economy*. Oxford University Press.
- Wardrop, J. G. (1952). Some theoretical aspects of road traffic research. In *Proceedings of the Institution of Civil Engineers*, volume 1, pages 325–362.
- Watling, D. (1999). Stability of the stochastic equilibrium assignment problem: a dynamical systems approach. *Transportation Research Part B: Methodological*, 33(4):281–312.
- Watling, D. and Hazelton, M. L. (2003). The dynamics and equilibria of day-to-day assignment models. *Networks and Spatial Economics*, 3(3):349–370.
- Weibull, J. W. (1997). *Evolutionary game theory*. MIT press.
- Xiao, F., Shen, M., Xu, Z., Li, R., Yang, H., and Yin, Y. (2019). Day-to-day flow dynamics for stochastic user equilibrium and a general lyapunov function. *Transportation Science*, 53(3):683–694.
- Xiao, L. and Lo, H. K. (2015). Combined route choice and adaptive traffic control in a day-to-day dynamical system. *Networks and Spatial Economics*, 15(3):697–717.
- Xie, J., Nie, Y., and Liu, X. (2018). A greedy path-based algorithm for traffic assignment. *Transportation Research Record*, 2672(48):36–44.
- Xie, J., Nie, Y. M., and Liu, X. (2017). Testing the proportionality condition with taxi trajectory data. *Transportation Research Part B: Methodological*, 104:583–601.
- Xu, Y., Xie, L., Zhang, X., Chen, X., Qi, G.-J., Tian, Q., and Xiong, H. (2019). Pc-darts: Partial channel connections for memory-efficient architecture search. *arXiv preprint arXiv:1907.05737*.
- Yang, H. (1995). Heuristic algorithms for the bilevel origin-destination matrix estimation problem. *Transportation Research Part B: Methodological*, 29(4):231–242.
- Yang, H. and H. Bell, M. G. (1998). Models and algorithms for road network design: a review and some new developments. *Transport Reviews*, 18(3):257–278.
- Yang, H., Sasaki, T., Iida, Y., and Asakura, Y. (1992). Estimation of origin-destination matrices from link traffic counts on congested networks. *Transportation Research Part B: Methodological*, 26(6):417–434.
- Yang, H., Zhang, X., and Meng, Q. (2007). Stackelberg games and multiple equilibrium behaviors on networks. *Transportation Research Part B: Methodological*, 41(8):841–861.
- Zhang, D. and Nagurney, A. (1996). On the local and global stability of a travel route choice adjustment process. *Transportation Research Part B: Methodological*, 30(4):245–262.
- Zhang, K. and Nie, Y. M. (2018). Mitigating the impact of selfish routing: An optimal-ratio control scheme (orcs) inspired by autonomous driving. *Transportation Research Part C: Emerging Technologies*, 87:75–90.
- Zhang, L., Lawphongpanich, S., and Yin, Y. (2009). An active-set algorithm for discrete network design problems. In *Transportation and Traffic Theory 2009: Golden Jubilee*, pages 283–300. Springer.
- Zhang, W.-y., Guan, W., Ma, J.-h., and Tian, J.-f. (2015). A nonlinear pairwise swapping dynamics to model the selfish rerouting evolutionary game. *Networks and Spatial Economics*, 15(4):1075–1092.